Small Structures

small structures

www.small-structures.com

REVIEW OPEN ACCESS

Vertically Aligned Micro- and Nanoneedles for Advanced Biomedical Applications: From Fabrication Strategies to Clinical Translation

Yerim Jang[1] | Sowon Lee[1,2] | Younghak Cho[3] | Hyejeong Seong[1,4]

[1]Brain Science Institute, Korea Institute of Science and Technology, Seoul, Republic of Korea | [2]Department of Bioengineering, Korea University, Seoul, Republic of Korea | [3]Department of Physiology, Anatomy and Genetics, Department of Engineering Science, Kavli Institute for Nanoscience Discovery, University of Oxford, Oxford, UK | [4]Division of Bio-Medical Science and Technology, University of Science and Technology, Seoul, Republic of Korea

Correspondence: Younghak Cho (younghak.cho@dpag.ox.ac.uk) | Hyejeong Seong (h.seong@kist.re.kr)

Received: 23 October 2025 | **Revised:** 14 January 2026 | **Accepted:** 16 January 2026

Keywords: biosensing | mechanobiology | nanofabrication | therapeutics | vertically aligned nanostructures

ABSTRACT

Effective therapeutic delivery and diagnostic monitoring at cellular levels are constrained by biological barriers including stratum corneum, extracellular matrix, and plasma membranes. Conventional approaches such as viral vectors and liposomes face limitations including inadequate penetration, immunogenicity, and invasiveness. High-aspect-ratio nanostructures, including nanoneedles and microneedles, address these challenges through their unique geometries enabling direct, minimally invasive cellular access. This review examines high-aspect-ratio nanostructure technologies from fabrication strategies to therapeutic and diagnostic applications. We discuss bottom-up synthesis, top-down lithographic methods, and integrative approaches enabling precise control over geometry, mechanical properties, and surface functionalization. Mechanotransduction applications reveal how these architectures modulate cellular behavior through mechanosensitive pathways and enable phenotypic control. Recent advances have expanded applications to precision medicine through intracellular delivery of genetic engineering tools to challenging cell populations including immune cells and neurons. Hollow, porous, and surface-functionalized architectures enable controlled therapeutic release and targeted cellular reprogramming. Diagnostic applications demonstrate capabilities for intracellular sensing and continuous physiological monitoring. Convergence with artificial intelligence promises adaptive, personalized therapeutic protocols. However, challenges including scalable manufacturing, long-term biocompatibility, and regulatory translation must be addressed to realize clinical potential. This review positions high-aspect-ratio nanostructures as foundational platforms for next-generation precision medicine and personalized healthcare.

1 | Introduction

Effective therapeutic interventions and diagnostic monitoring at the cellular and subcellular levels remain fundamental challenges in modern biomedicine. Biological barriers, including the stratum corneum, extracellular matrix (ECM), and cellular membranes, severely restrict the delivery of macromolecular therapeutics and prevent direct access to intracellular compartments for real-time molecular sensing [1, 2]. Conventional drug-delivery approaches using agents such as viral vectors and liposomes show critical limitations, including restricted cargo capacity, inadequate control over intracellular trafficking, potential immunogenicity, and limited ability to target specific cell populations [3]. Similarly, traditional diagnostic methods lack the spatiotemporal resolution necessary to monitor dynamic intracellular processes, limiting their ability to characterize disease mechanisms and facilitate optimization of therapeutic

This is an open access article under the terms of the Creative Commons Attribution License, which permits use, distribution and reproduction in any medium, provided the original work is properly cited.

© 2026 The Author(s). *Small Structures* published by Wiley-VCH GmbH.

responses at the single-cell level. These fundamental limitations necessitate the development of alternative technologies than can bypass biological barriers while maintaining cellular viability and physiological functions.

To overcome these challenges, micro- and nanoneedle structures, which are characterized by their high aspect ratios and precisely engineered needle-like geometries, have emerged as transformative platforms for biointerface engineering over the past two decades. These geometries enable unique physical interactions with biological systems at both cellular and subcellular levels, creating opportunities for controlling fundamental biological processes. The capacity of these structures to directly interface with living cells while preserving cellular viability has positioned them at the leading edge of diverse biomedical applications, ranging from mechanotransduction studies [4, 5] to advanced therapeutic-delivery systems. However, before examining how these capabilities are realized through advanced fabrication techniques, establishing a clear operational definition of a 'high-aspect-ratio nanostructure' is essential.

In this review, high-aspect-ratio nanostructures are operationally defined as vertical structures with aspect ratios (height/base diameter) ≥10, a threshold that distinguishes these architectures from low-aspect-ratio planar nanostructures (e.g., nanodots, nanogrooves; aspect ratio <5) with fundamentally different cellular interface behaviors. This geometric criterion encompasses structures spanning both nanoscale (base diameter: 10 nm to 1 μm) and microscale (base diameter: 1–1000 μm) dimensions. Nanoscale structures, including nanoneedles, nanopillars, and nanowires, typically exhibit higher aspect ratios (AR = 50–100) and allow single-cell interfacing with subcellular resolution, whereas microscale structures, such as microneedles, generally have moderate aspect ratios (AR = 10–50) optimized for tissue-level applications, including transdermal delivery and biosensing. The unifying feature across these dimensional regimes is their vertical needle-like geometry, which creates localized mechanical interactions with biological membranes through similar biophysical mechanisms, such as membrane deformation, penetration, and transient permeabilization, regardless of the absolute size. This review encompasses both scales to provide a comprehensive coverage of high-aspect-ratio architectures for biomedical applications, while explicitly noting dimensional distinctions that are relevant for specific applications.

To provide a systematic framework for understanding how structural dimensions determine biological accessibility and therapeutic applicability, Table 1 presents a length-dependent classification of vertically aligned micro- and nanoneedle platforms. This length-based framework serves as a conceptual foundation for the fabrication strategies (Section 2), cellular applications (Section 3), therapeutic-delivery systems (Section 4), and diagnostic platforms (Section 5) discussed in this review.

The realization of these unique capabilities has been enabled by remarkable advances in nanofabrication techniques that provide precise control over critical structural parameters, including morphology [15], tip sharpness [16, 17], spatial arrangement [18], and surface porosity [19]. This level of architectural control allows researchers to tailor nanostructures for specific applications and create optimized structures for specific biological interactions. Engineering these parameters with nanoscale precision has unlocked capabilities that were previously inaccessible with conventional biomedical devices, thereby establishing high-aspect-ratio nanostructures as a unique class of biointerface materials with tunable physical and chemical properties.

These advances in fabrication have enabled diverse biomedical applications that leverage the unique interfacing capabilities of high-aspect-ratio nanostructures. Their capacity to penetrate biological barriers, including the skin, ECM, and mucus layer, with minimal tissue disruption addresses the fundamental limitations of conventional drug-delivery methods, which often show poor permeability and inadequate efficacy in transporting macromolecular therapeutics across biological membranes [20]. By enabling efficient intracellular delivery of therapeutic agents into the cytosolic and nuclear compartments, high-aspect-ratio nanostructures offer compelling alternatives to traditional delivery systems. Moreover, the functionality of these nanostructures can be further enhanced through physical and chemical

TABLE 1 | Length-dependent classification of nano- and microneedle systems and their biomedical applicability.

Categories		Length (AR)	Penetration depth	Primary biological targets	Ref
Nanoscale	Intracellular delivery (CRISPR, siRNA) Mechanotransduction Single cell biosensing	0.5–10 μm (10–100)	<1 μm (affecting membrane, nuclear envelope)	Single cells, intracellular compartments (cytosols, nucleus)	[6, 7]
Low-microscale	Localized delivery Wound healing Neural guidance	10–100 μm (10–50)	10–300 μm	Viable epidermis, superficial dermis, dense connective tissues (disc, cartilage)	[8–11]
High-microscale	Transdermal delivery Systemic microneedles (contraceptions, vaccines) Cancer immunotherapy (CAR-T) Continuous monitoring	100–1000 μm (2–20)	300–1500 μm	Dermis, subcutaneous tissue	[12–14]

modifications, including targeted surface functionalization [21, 22], synergistic electroporation [6], and vibration-assisted membrane penetration [23], yielding multifunctional platforms with precisely tunable properties.

In addition to their therapeutic-delivery applications, these structures have demonstrated great potential as advanced biosensing platforms. Their high surface-area-to-volume ratios facilitate efficient functionalization with biomolecular recognition elements, enabling rapid, localized, and precise detection of intracellular markers in real time [24]. In particular, recent advances have highlighted the potential of these nanostructures to deliver next-generation genetic engineering tools to challenging cell types, including immune cells and neurons [7, 25]. Despite these advances, however, comprehensive reviews encompassing the full spectrum of high-aspect-ratio nanostructure applications, particularly recent advancements in clinical translation, advanced therapeutic-delivery mechanisms, and integrated diagnostic platforms, remain limited. Although previous reviews have addressed specific aspects, such as fabrication methods or mechanotransduction applications [26, 27], a holistic analysis connecting fundamental cellular interactions to clinical translation pathways is lacking. This gap is particularly relevant given the rapid evolution of precision medicine and the emergence of artificial intelligence (AI)-integrated nanostructured platforms.

To address this gap, the present review provides an integrated analysis of recent advancements in the nanostructure technology landscape, with a specific focus on fabrication strategies, mechanobiological applications, therapeutic-delivery systems, and diagnostic platforms. We examine how structural design principles and material composition influence performance across diverse applications while critically assessing existing technological challenges. We explore the transition from fundamental cellular studies to high-throughput, clinically applicable systems and discuss emerging opportunities in AI-integrated platforms for personalized medicine. Finally, we propose research priorities with quantifiable milestones that can accelerate the translation from laboratory innovations to clinical solutions, ultimately advancing the field toward patient-specific therapeutic interventions.

2 | Fabrication Strategies for Vertically Aligned, High-Aspect-Ratio Micro-/Nanoneedle Structures

Engineering of high-aspect-ratio nanostructures is a critical frontier in the field of biomedical nanotechnology. The aspect ratio, which is defined as the ratio of the structural length to the base diameter, governs both mechanical integrity and biological functionality. Unlike planar nanostructures, such as grooves or dots [28, 29], high-aspect-ratio structures must achieve a delicate balance between extreme slenderness and sufficient robustness to penetrate cellular membranes without mechanical failure. Contemporary fabrication strategies can be categorized as bottom-up and top-down strategies (Figure 1), each of which offers distinct advantages for specific applications within nanostructure-biosystem interfaces.

2.1 | Bottom-Up Fabrication

In bottom-up fabrication, high-aspect-ratio structures are constructed from atomic or molecular precursors, enabling precise control over the nanoscale dimensions and composition. This approach conceptually mirrors the natural growth processes and builds complex structures through controlled assembly rather than material removal.

CVD, particularly through the vapor–liquid–solid (VLS) mechanism [30], represents one of the most widely adopted techniques

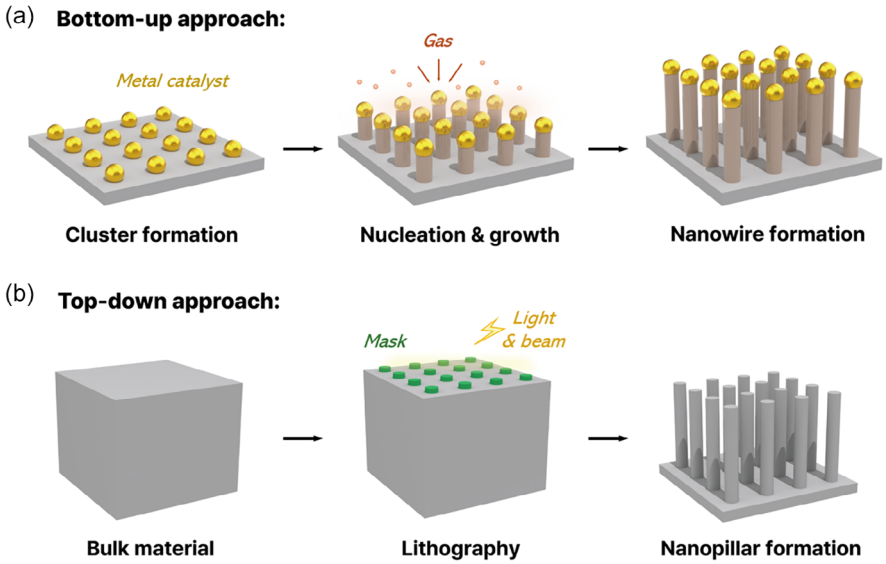

FIGURE 1 | Schematic representation of the bottom-up and top-down approaches for fabricating high-aspect-ratio nanostructures. (a) The bottom-up approach, represented by chemical vapor deposition (CVD) with vapor–liquid–solid (VLS) growth, assembles structures from atoms or molecules through three stages: metal catalyst clustering, gas-phase nucleation and epitaxial growth, and final nanowire formation, allowing precise nanoscale control. (b) The top-down approach, represented by lithography combined with etching, shapes structures by removing material from bulk substrates through patterning (using photomasks or electron beams) and subsequent etching processes. Detailed procedures for the lithographic methods (photolithography, electron-beam lithography, nanoimprint lithography) and etching technologies (wet and dry etching) are described in Section 2.2.

in this category. In this process, catalytic nanoparticles (typically gold [Au]) facilitate the nucleation and epitaxial growth of nanostructures from gaseous precursors [31]. The metal catalyst forms a liquid eutectic with the target material, allowing continuous precipitation and crystallization of the precursor gases that dissolve in the liquid phase. This process offers remarkable control over multiple structural parameters simultaneously; the nanowire diameter is governed by the catalyst particle size, length by growth duration, and composition by precursor gas ratios.

Kwon et al.. demonstrated this precise control by systematically modulating Au nanoparticle characteristics and growth conditions to produce silicon nanowires with base diameters of several hundred nanometers and heights approaching 2 μm [32]. Their work exemplified the dimension control achievable through optimized VLS growth processes.

Template-assisted synthesis is another powerful bottom-up strategy, particularly for fabricating hollow nanostructures such as nanostraws. This approach involves depositing materials onto predefined nanoscale templates, such as porous anodic aluminum oxide (AAO) membranes or track-etched polycarbonate (PC) membranes, which serve as scaffolds for material deposition. Deposition can occur through template-based CVD synthesis [33] or atomic layer deposition (ALD), with the latter offering unprecedented precision.

ALD achieves atomic-level control through a self-limiting surface reaction mechanism, wherein precursors react only with the previously formed monolayer, enabling layer-by-layer growth with subnanometer precision [34]. Liu et al.. leveraged this capability to create alumina-based hollow nanoneedles by depositing precisely controlled alumina layers onto PC membranes, which was followed by selective template removal [7]. The resulting nanostraws exhibited uniform wall thickness and dimensional characteristics, which are ideal for high cargo-loading capacity and cellular-delivery applications.

Although bottom-up approaches provide exceptional control over nanostructure morphology and scalability for complex architectures, they show limitations in terms of spatial uniformity and mechanical robustness. The stochastic nature of the nucleation processes can lead to heterogeneity in nanostructure positioning and dimensions across a substrate. Additionally, the crystalline nature of such bottom-up synthesized structures can yield anisotropic mechanical properties that may compromise resilience during cellular insertion. These limitations have driven researchers toward top-down fabrication methods for applications that require precise spatial control and enhanced mechanical stability [7, 24, 34].

2.2 | Top-Down Fabrication

In the top-down fabrication approach, defined nanostructures are created through selective removal of materials from bulk substrates. The general process flow consists of two fundamental steps: (1) lithographic patterning to define the spatial arrangement of structures and (2) etching to create 3D architectures by removing unprotected material.

2.2.1 | Lithographic Approaches

Photolithography is a widely employed lithographic technique that transfers patterns from photomasks to photosensitive resists through controlled light exposure. Despite offering exceptional throughput and established integration with semiconductor manufacturing, conventional photolithography shows resolution limitations imposed by optical diffraction. Even with deep-ultraviolet (UV) light sources, feature sizes typically remain above 100 nm, limiting applications to moderately sized, highly aligned nanostructure arrays [35].

Electron-beam lithography (EBL) overcomes this resolution limitation by employing a focused electron beam to directly write nanoscale patterns onto electron-sensitive resists. The de Broglie wavelength of the accelerated electrons (10–100 keV) falls within the picometer range, allowing pattern definition below 10 nm under optimized conditions [36]. This exceptional resolution has made EBL invaluable for prototyping high-precision nanostructure arrays [17, 37–40]. Despite its resolution advantages, the serial writing processes in EBL, wherein patterns must be traced sequentially rather than exposed simultaneously, imposes substantial throughput limitations and high operational costs. As a result, EBL primarily serves as a research tool or an approach for creating master templates rather than a method for high-volume production.

2.2.2 | Etching Technologies

After lithographic patterning, etching processes selectively remove materials to create 3D high-aspect-ratio nanostructures. Etching approaches for nanostructure fabrication can be categorized as wet etching (using liquid etchants) or dry etching (using reactive gas-phase species) [41], with each approach offering distinct advantages for specific applications.

The wet-etching method provides procedural simplicity, low equipment costs, and high material selectivity. Electrochemical etching (ECE) is a sophisticated wet-etching technique that uses controlled electrical currents to modulate metallic surface dissolution with exceptional precision. Hussein et al.. used this approach to fabricate silver (Ag) probes with precisely controlled tip geometries by systematically adjusting the electrochemical parameters in perchloric acid ($HClO_4$) solution [42]. By balancing the competing oxide formation and dissolution kinetics, they achieved remarkable control over the tip profile and surface smoothness.

Metal-assisted chemical etching (MACE) is another well-established wet-etching method for fabricating silicon-based porous nanostructures. This catalytic process employs noble metal catalysts (e.g., Au or Ag) to locally accelerate silicon etching in the presence of hydrogen peroxide and hydrofluoric acid. Metal nanoparticles function as nanoscale galvanic cells, creating anisotropic etching pathways that follow the movement of the catalyst. Wang et al. demonstrated the versatility of MACE by precisely adjusting etching parameters to produce silicon nanoneedles with controlled dimensions and porosity gradients [43]. This makes MACE a valuable approach for creating biodegradable nanostructure platforms [19, 20].

Although wet etching offers numerous advantages, it is frequently limited in terms of anisotropy and spatial resolution. The diffusion-limited nature of most wet-etching processes yields isotropic profiles and results in undesirable lateral undercutting, compromising high-aspect-ratio structures. To address this limitation, dry-etching methodologies are preferred for high-precision fabrication of nanostructures.

Reactive ion etching (RIE) is the gold standard dry-etching technique for creating high-aspect-ratio nanostructures with exceptional anisotropy. RIE combines chemical etching by reactive plasma species with physical bombardment by directional ions, creating highly anisotropic profiles that maintain pattern fidelity even at extreme aspect ratios [17, 23, 24, 43, 44]. For silicon-based nanoneedles, deep reactive ion etching (DRIE) implemented through the Bosch process, which alternates between etching and sidewall passivation steps, yields aspect ratios exceeding 50:1, enabling extremely slender nanoneedles with sufficient mechanical integrity for cellular applications [20].

Despite their remarkable capabilities, conventional lithography and etching techniques show limitations in terms of surface damage, equipment cost, and processing complexity. These constraints have motivated alternative fabrication strategies that reduce process complexity while maintaining nanoscale precision.

2.2.3 | Nanoimprint Lithography

Nanoimprint lithography (NIL) has emerged as a particularly promising alternative that combines nanoscale resolution and high-throughput processing. NIL employs prepatterned templates to physically deform soft resist materials, creating pattern transfers with nanoscale fidelity. The deformed resist can be cured using thermal or UV processes to create stable structures. By utilizing soft and biocompatible materials such as polyurethane acrylate (PUA) [45], poly lactic acid (PLA) [46], SU-8 photoresist [47], and polydimethylsiloxane (PDMS) [48], NIL allows direct fabrication of polymeric high-aspect-ratio nanostructures with tunable mechanical properties.

The principal advantage of NIL lies in the combination of nanoscale resolution with parallel processing, which is suitable for high-volume production [49, 50]. Unlike serial techniques such as EBL, NIL simultaneously transfers entire pattern fields across wafer-scale substrates, yielding throughput improvements of several orders of magnitude while maintaining feature definition below 10 nm under optimized conditions [51]. This combination positions NIL as a transformative approach for translational nanostructure development, bridging laboratory prototyping and clinical-scale manufacturing [45, 52].

Beyond NIL, alternative fabrication strategies, including the ice-templating method [12], direct/indirect 3D printing [8, 53], and micro-molding techniques [9, 13, 54], which primarily employ polymeric materials, have also been explored to produce microneedles for in vivo applications. However, these approaches are generally limited to the fabrication of microscale structures and may lack the precision required for true nanoscale features. Selection of an appropriate fabrication method on the basis of the desired structural and functional characteristics is crucial for optimizing the performance and applicability of high-aspect-ratio platforms in various biomedical applications.

2.3 | Integrative Approaches

The continuing evolution of nanoneedle fabrication has increasingly led researchers toward integrative approaches that transcend the traditional dichotomy between bottom-up and top-down methodologies. These hybrid strategies selectively combine elements from multiple fabrication paradigms to overcome the inherent limitations of individual techniques. One promising hybrid approach combines lithographic patterning with template-assisted synthesis by using deterministically defined template structures as scaffolds for material deposition through bottom-up processes [55]. This strategy maintains the spatial precision of top-down approaches while incorporating the atomic-scale compositional control offered by bottom-up methods [56, 57].

Another emerging direction involves post-fabrication surface modification of lithographically defined nanostructures through bottom-up chemical processes to engineer the surface properties without altering the underlying mechanical structure [58]. These approaches include functional polymer grafting to enhance cellular interactions [59]. nanoscale coating deposition to improve biosensing properties [60], and the incorporation of nanocoating for targeted delivery applications [21].

The selection of a fabrication methodology for high-aspect-ratio nanostructure platforms ultimately requires careful consideration of multiple factors, including the desired dimensions, material requirements, mechanical-performance requirements, surface-functionality requirements, production-volume expectations, and economic constraints. Each approach offers unique advantages and limitations for specific applications within a broader nanostructure landscape (Figure 2). As the field continues to mature, integrative approaches that selectively combine the strengths of different fabrication paradigms are likely to emerge as the dominant strategies for creating next-generation nanoneedle platforms tailored for specific biomedical applications.

2.4 | Material Selection Strategies

Material selection plays a pivotal role in determining the mechanical performance, biological interactions, and translational feasibility of high-aspect-ratio nanostructures [63, 64]. Beyond geometric parameters, intrinsic material properties govern the insertion efficiency, cellular response, degradation behavior, and compatibility with specific biomedical applications [65–67]. To date, silicon, metals, polymers, and hybrid systems have been employed, each offering distinct advantages for particular applications.

Silicon-based platforms are the most extensively studied class, offering exceptional mechanical stiffness (Young's modulus: 130–180 GPa) [68, 69], and precise fabrication control through established semiconductor processes [17, 18, 70]. Anisotropic etching can yield atomically sharp tips (<10 nm) that ensure reliable membrane penetration while minimizing cellular damage [16, 71]. A key advantage of this approach is the tunable biodegradability through controlled porosity engineering; porous silicon structures degrade predictably in physiological environments, and their degradation rates can be adjusted to span from days to months by varying the porosity (10%–80%) [72]. This combination of mechanical precision and controlled degradation makes silicon particularly suitable for applications requiring sustained structural integrity followed by complete resorption. However, the brittleness and optical opacity of silicon

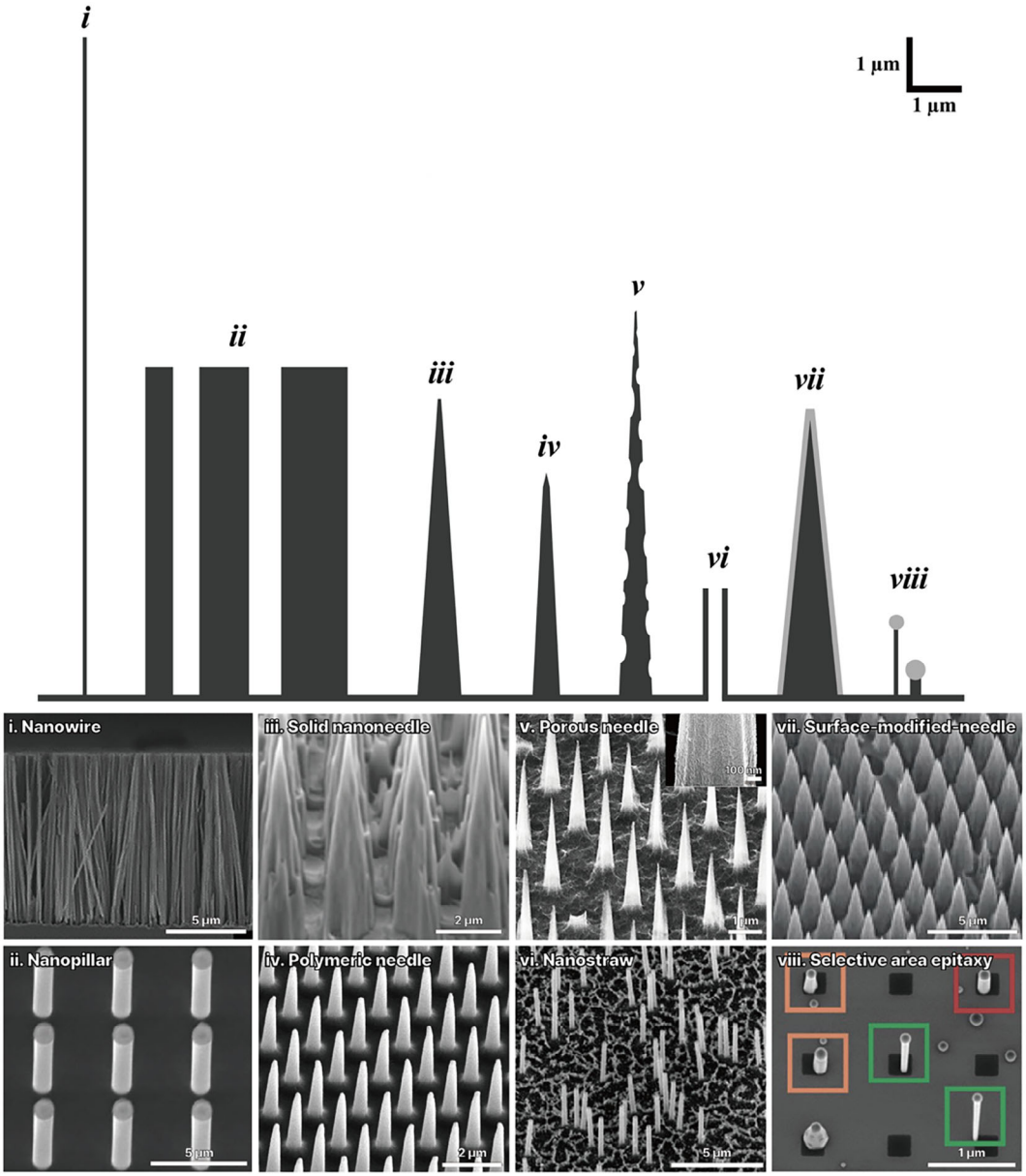

FIGURE 2 | Representative examples of vertical micro- and nanoneedle structures. (i–viii) Schematic depiction of various needle structures drawn to the same scale; (i) Nanowire: 200 nm base diameter, 18 µm height, aspect ratio (AR) = 90. Reproduced with permission [22]. Copyright 2019, American Chemical Society. (ii) Nanopillar: 500 nm base diameter, 5–6 µm height, AR = 10–12. Reproduced with permission [61]. Copyright 2024, Wiley. (iii) Solid needle: 800 nm base diameter, 5 µm height, AR = 6.25. Reproduced with permission [62]. Copyright 2018, The Authors, published by American Association for the Advancement of Science. (iv) Polymeric needle: 539 nm base diameter, 3.8 µm height, AR = 7. Reproduced with permission [45]. Copyright 2025, Nature Springer. (v) Porous needle: 600 nm base diameter, 5–7 µm height, AR = 8–12. Reproduced with permission [43]. Copyright 2024, The Authors, Published by American Chemical Society. (vi) Nanostraw: 200 nm base diameter, 2 µm height, AR = 10. Reproduced with permission [7]. Copyright 2024, Wiley. (vii) Surface modified nanoneedle: 700–800 nm base diameter, 4.5 µm height, AR = 5–6. Reproduced with permission [21]. Copyright 2022, Wiley. (viii) Selective area epitaxy nanowire: thick region 200 nm diameter/400 nm height, thin region 70–100 nm diameter/800–1400 nm height, AR = 2–14. Reproduced with permission [56]. Copyright 2021, American Chemical Society. Note that structures (i), (ii), and (vi) with AR $\geq$ 10 represent the high-aspect-ratio architectures that are the primary focus of this review, while the other structures are included for comparative context to illustrate the broader landscape of vertical needle structures.

as well as the cleanroom fabrication requirements for working with silicon limit its applicability in flexible devices and constrain manufacturing scalability.

Metallic structures, including gold, silver, and stainless steel, offer complementary advantages for applications requiring high electrical conductivity or extreme mechanical robustness [73–80]. For instance, gold nanoneedles combine excellent biocompatibility with superior electrical properties, making them ideal for multielectrode arrays for electrophysiological recording and neural interfacing [75, 76]. However, most metals lack biodegradability, raising concerns regarding long-term tissue accumulation [73, 81]. This factor limits the clinical applicability of metallic nanostructures primarily to research tools rather than implantable therapeutics.

Polymeric structures have emerged as the most clinically advanced platforms, offering superior biocompatibility, tunable biodegradability, and scalable manufacturing. The use of Food and Drug Administration (FDA)-approved biodegradable polymers (PLA and poly(lactic-co-glycolic) acid [PLGA]) can allow complete resorption without surgical removal, thereby addressing the critical safety concerns associated with long-term implantable devices [82, 83]. The degradation rates of these polymers can be precisely tuned by adjusting the copolymer composition (PLA:PGA ratio) and molecular weight, yielding customized release profiles spanning from days to months. Recent advancements have expanded the polymeric capabilities through stimuli-responsive systems that respond to physiological cues for intelligent drug release. For example, temperature-responsive poly(*N*-isopropylacrylamide) (PNIPAm) undergoes phase transitions at body temperature for thermally triggered release, whereas pH-responsive formulations allow visual infection monitoring coupled with acidification-triggered antibiotic release [84]. Self-healing polymers show enhanced in vivo durability while maintaining biocompatibility [85, 86], preventing premature degradation and enabling precise temporal control. These advances have led to commercial success in applications such as transdermal vaccine delivery and wound healing, where patient comfort, self-administration, and high-volume manufacturing are paramount [87].

Since no single material optimally addresses all requirements, hybrid and multifunctional systems that combine the complementary advantages of different material classes have also been developed. For example, surface-modification strategies can create ultrathin biodegradable polymer coatings on rigid silicon or metallic nanostructures, incorporating stimuli-responsive elements while preserving the sharp geometry [21, 22]. More sophisticated approaches include magnetoresponsive microneedles that integrate polymeric matrices with embedded magnetic nanoparticles, allowing remote actuation and spatiotemporal control of both insertion depth and drug release [66]. These hybrid designs exemplify how material integration can achieve functionalities unattainable through single-material platforms.

Advanced micro-/nanoneedle concepts have also emerged to address specialized biomedical challenges. Cryomicroneedles employ cryoprotectant-loaded or ice-templated structures that maintain subzero temperatures during insertion, thereby protecting temperature-sensitive biologics, including live cells, proteins, and mRNA therapeutics [12, 65]. This approach has proven to be particularly valuable for cell-based immunotherapies, where maintaining viability during delivery is critical. Similarly, antioxidant microneedles incorporate radical scavengers directly into structural matrices, providing dual functionality, i.e., mechanical delivery combined with inherent therapeutic activity, which is particularly valuable for diabetic wound healing, where oxidative stress impairs repair [88]. For regenerative applications, bioactive materials, including natural polymers, ceramics, and carbon-based nanomaterials, offer enhanced osteoconductivity and tissue integration [64]. Meanwhile, conductive polymers can enable combined electrical stimulation and drug delivery, thereby advancing neural tissue engineering and cardiac applications [89].

The diversity of available materials and architectures has necessitated application-specific selection, which balances often-competing requirements. Thus, for intracellular delivery, silicon or sharp metallic nanostructures (aspect ratio >50) with biodegradable coatings ensure reliable membrane penetration and controlled drug release. For transdermal delivery, biodegradable polymers (PLA and PLGA) provide patient comfort and safety with moderate aspect ratios (10–20) sufficient for stratum corneum penetration. For biosensing, conductive materials (gold and conductive polymers) enable signal transduction while maintaining mechanical flexibility for chronic implantation. The use of cryoprotective materials with an open architecture for immunotherapy and cell-based therapies can facilitate cell viability, migration, and retention [67]. Multifunctional hybrid systems that strategically combine materials increasingly represent the most promising approach for translating nanostructure technologies into clinical practice, since they overcome the limitations of single-material platforms while being optimized for specific biomedical applications. This trend toward material integration reflects the field's maturation from proof-of-concept demonstrations to clinically viable, application-tailored therapeutic systems.

A comparative overview of the bottom-up, top-down, and integrative fabrication approaches for vertically aligned micro- and nanoneedles is provided in Table 2, which highlights their key process characteristics and practical considerations.

3 | Classical Applications of High-Aspect-Ratio Nanostructures: Cellular Applications

The vertical geometry of high-aspect-ratio nanostructures creates a unique biophysical interface that fundamentally alters the interactions between the cells and their environments. When cells encounter these nanostructures, they experience localized mechanical perturbations that trigger complex cellular responses through mechanotransduction pathways, which are biological processes by which mechanical stimuli are converted into biochemical signals. This cell–nanostructure dialog is extremely sensitive to geometric parameters, including structure shape [16, 95, 96], density [15, 18], height [97], and material stiffness [47, 98], allowing for precise modulation of cellular behavior through purely physical cues. At this specialized interface, cells respond to nanostructures through active membrane adaptation, including bending [99, 100] and wrapping [37] around the vertical tips, which creates localized regions of high membrane curvature that serve as initiation sites for mechanosensitive signaling cascades.

These nanoneedle-induced deformations represent more than a passive cellular response; they constitute active mechanosensing events that orchestrate changes in the cellular architecture and function [101]. Through mechanotransduction, these physical interactions activate diverse signaling networks that regulate fundamental cellular processes, including proliferation [45, 84], migration [37], alignment [32, 89], and differentiation [28, 102–105]. This section explores the multifaceted interactions between cells and nanostructures, examining how these structures both probe and modulate cellular mechanics (Section 3.1), activate specific mechanotransduction pathways to regulate cellular behavior (Section 3.2), and ultimately direct cell phenotype determination through mechanical programming (Section 3.3).

TABLE 2 | Overview of bottom-up, top-down, and integrative nanoneedle fabrication strategies.

Fabrication approach	Technique	Structural control	Main advantages	Typical limitations	Ref.
Bottom-up	CVD (VLS)	Nanowire diameter and composition governed by catalyst nanoparticle size and precursor chemistry	- Nanometer-scale diameter and compositional tunability	- Stochastic positioning and size dispersion - Anisotropic mechanical properties	[31, 32]
	Template-assisted (CVD/ALD)	Template pore diameter and length define geometry; ALD cycles control wall thickness	- Uniform hollow nanoneedles - High cargo-loading capacity	- Additional steps for template fabrication and removal	[7, 34, 70]
Top-down	Photolithography (UV) + etching	Photomask defines pitch and layout; feature size typically > 100 nm	- Highly aligned nanostructure arrays - High scalability and reproducibility	- Resolution limited by optical diffraction	[35]
	EBL + etching	Direct-write electron beam patterning enables sub-10 nm feature definition	- Ultimate patterning precision - Flexible design capability	- Extreme low throughput - High operational cost	[17, 36–40]
	Wet etching (ECE, MACE)	Electrochemical parameters or metal catalysts tune tip geometry and porosity	- Precise control of tip geometry and porosity - Simple and cost-effective processing	- Limited anisotropy - Lateral undercutting constrains achievable aspect ratios.	[19, 20, 42, 43]
	Dry etching (RIE, DRIE)	Plasma chemistry and ion bombardment control sidewall profile and aspect ratio	- Highly anisotropic etching enables very high-aspect-ratio nanoneedles	- Potential plasma-induced surface damage - Complex and expensive equipment	[17, 20, 23, 24, 43, 44]
	NIL	Pre-patterned template molds define replicated nanostructures with nanoscale fidelity	- Nanoscale resolution with high-throughput, large-area fabrication - Compatible with soft and biocompatible polymers	- Requires durable master molds - Mechanical robustness depends on polymer properties	[45–49, 51, 52, 90, 91]
Integrative	Hybrid fabrication and post-modification	Lithography defines geometry, while bottom-up coatings or grafting tune surface functionality	- Combines spatial precision with versatile surface and functional control	- Increased process complexity - Potential coating stability issues	[21, 55, 56, 60, 92–94]

3.1 | Enhanced Cell-Chip Coupling and Probing Cellular Mechanics

The interface between living cells and high-aspect-ratio nanostructures represents a dynamic mechanical junction that fundamentally alters the cellular architecture while providing unprecedented access to intracellular compartments. When cells encounter high-aspect-ratio nanostructures, they undergo complex mechanical adaptations involving coordinated plasma membrane and nuclear deformation. These deformation modalities manifest as direct membrane penetration [106, 107], transient membrane permeabilization [108], or active endocytosis [47, 109] (Figure 3). The predominant interaction mechanism depends on a complex interplay between nanostructure geometry, material properties, and cell-specific characteristics, creating a tunable system for investigating and manipulating cellular mechanics.

Advanced imaging techniques have revealed the intricate nanoscale architecture of these cell–nanostructure interfaces. Correlative microscopic approaches combining scanning electron microscopy (SEM) [47, 72], focused ion beam scanning electron microscopy (FIB-SEM) [71, 114, 115], and fluorescence imaging [116, 117] have revealed the 3D organization of these interactions with unprecedented resolution. At the cell surface, adherent cells cultured on vertical nanostructures exhibit distinct morphological adaptations, including flattened and elongated profiles with filopodial extensions actively anchored to the structures [115], creating mechanically linked structures that vary significantly across different cell types [15, 47]. These surface adaptations reflect deeper intracellular reorganization; for example, Chen et al. used FIB-SEM to reveal that silicon nanowires can simultaneously induce both direct membrane penetration and active endocytic engulfment, with intracellular vesicle formation around nanowires confirming sophisticated cellular responses to these mechanical challenges [113].

The ability of vertical nanostructures to transiently permeabilize cellular membranes has emerged as a particularly valuable characteristic for biomedical applications. These structures, which range from solid architectures to hollow conduits, generate highly localized mechanical stress at the plasma membrane, creating nanoscale pores that enable bidirectional molecular transport while preserving overall cellular viability. This form of controlled disruption facilitates both targeted intracellular delivery of therapeutic cargoes and extraction of cellular contents for analytical applications, while simultaneously enabling high-resolution electrophysiological monitoring of multiple cells [21, 118]. Remarkably, Sarikhani et al. demonstrated that even vertical nanostructures that are simply engulfed by the cellular membrane without direct penetration can induce transient breaches in the nuclear envelope [119]. Their investigations revealed that membrane curvature alone can trigger nuclear poration events, with smaller nanopillars (height, 3.15 μm) proving more effective than larger nanopillars (height, 2.24 μm) at inducing nuclear envelope disruptions due to their higher curvature; this finding highlights the exquisite sensitivity of nuclear mechanics to plasma membrane deformation.

Nanostructure-induced membrane perturbations offer even greater precision and improved functionality when combined with complementary physical stimuli, particularly electrical forces. Xie et al. demonstrated this synergistic approach by employing vertical nanopillar electrodes and electrical stimulation to detect subtle action potential fluctuations in cardiomyocytes with exceptional signal-to-noise ratios [108]. Their assessments using time-resolved imaging revealed complete nanopillar engulfment by the cell membrane followed by rapid resealing within 10 min, demonstrating the remarkable adaptability of cellular membranes to these mechanical interventions and establishing a stable bioelectronic interface for longitudinal monitoring.

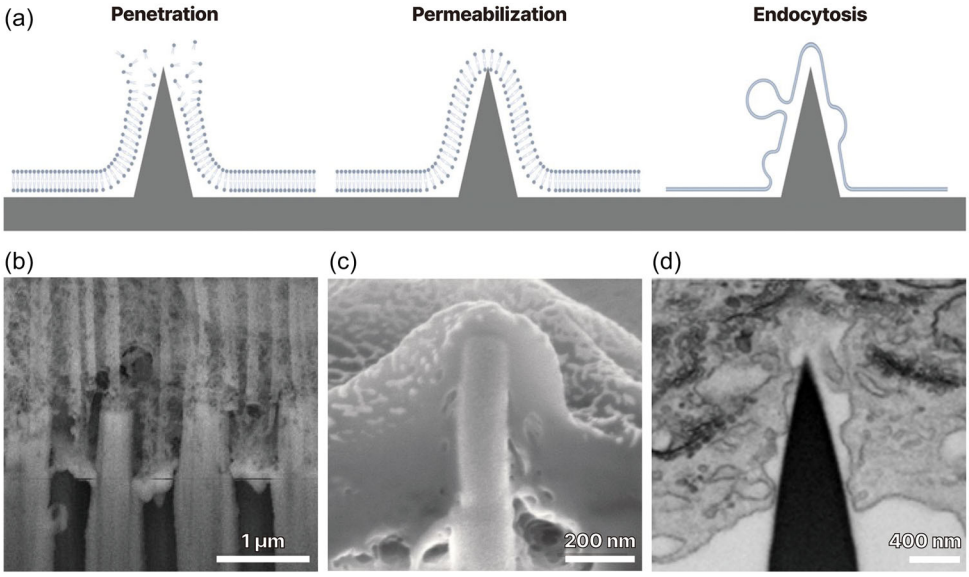

FIGURE 3 | Three representative modalities of cell-nanostructure interface: (a) Schematic of interaction mechanisms in the process of nanostructures' intracellular access. Reproduced with permission [110]. Copyright 2020, Wiley. (b) Mechanical penetration. Reproduced with permission [111]. Copyright 2015, Wiley. (c) Membrane permeabilization. Reproduced with permission [112]. Copyright 2018, American Chemical Society. (d) Endocytosis. Reproduced with permission [113]. Copyright 2020, American Chemical Society.

Beyond the plasma membrane effects, vertical nanostructures influence nuclear architecture, which is a critical determinant of gene expression and the cellular phenotype. The nuclear envelope, which consists of a double-lipid bilayer reinforced by a nuclear lamina, receives mechanical signals from the cell periphery through an intricate force transmission system involving actin cap—specialized actomyosin filaments that connect focal adhesions (FAs) at the cell surface to the nuclear membrane [120, 121]. This mechanical coupling creates a direct pathway for nanostructure-induced deformations to propagate to the nucleus, with vertical structures actively pulling the nuclear membrane into distinctive topographical conformations that dynamically appear and disappear as the cells remodel their cytoskeletons [122].

Pan et al. demonstrated precise control over nuclear morphology using poly(lactide-co-glycolide) micropillars with systemically varied heights (0–5 μm) [97]. By tailoring the micropillar patterns to accommodate nuclear dimensions and mechanical properties, they achieved programmable nuclear geometries, generating defined shapes, including squares and triangles, when a sufficient pillar height was present. This approach was extended to modulate human osteosarcoma U2OS and human mesenchymal stem cell (hMSC) morphologies on nanopillars and thereby create diverse nuclear configurations with variable roundness characteristics [123]. Quantitative analysis revealed significantly enhanced endocytic activity on the nanopillars when the cells were cultured on rectangular patterns exhibiting greater elongation, establishing a direct link between nuclear deformation and membrane-trafficking processes.

3.2 | Modulating Cell Behavior through Topography and Mechanotransduction Pathways

High-aspect-ratio nanostructures create unique mechanical microenvironments that cells actively sense and respond to through sophisticated mechanotransduction machinery. These structures function not only as passive topographical elements but also as active signaling hubs that convert mechanical interactions at the cell–nanostructure interface into biochemical signals that orchestrate fundamental cellular behaviors, including adhesion dynamics, migration patterns, and lineage commitment. By elucidating the molecular mechanisms through which vertical topographies influence signal transduction networks, researchers have established nanomechanical control over cellular functions with unprecedented precision (Figure 4).

At the molecular level, curvature-sensing proteins serve as the primary mechanosensors that detect and respond to the nanoscale membrane deformations induced by nanostructures. Formin-binding protein 17 (FBP17), a member of the F-BAR domain protein family, can detect membrane curvatures with diameters below 400 nm and subsequently activate downstream effectors, including neuronal Wiskott-Aldrich syndrome protein (N-WASP), cortactin, and the actin-related protein 2/3 (Arp2/3) complex to nucleate branched F-actin networks [124]. Remarkably, proteins without established curvature-sensitive domains, including adaptor protein 2 (AP2), intersectin, cortactin, and actin, also preferentially assemble at the highly curved membrane regions generated by nanostructural interactions [109]. These findings reveal how nanostructures initiate signaling cascades through geometric perturbations, triggering comprehensive cellular responses, including cytoskeletal reorganization [37, 124], nuclear envelope remodeling [16, 17], and activation of transcriptional regulators that control gene expression programs.

The specific dimensional characteristics of nanostructures critically influence the downstream cellular responses by creating distinct patterns of membrane deformation. Seong et al. demonstrated that sharp-tipped silicon nanoneedles (~54 nm in diameter) induce highly localized membrane indentation and wrapping. In contrast, the blunter pillar nanostructures (diameter, ~750 nm) promote broader membrane bending without complete engulfment [16]. These geometrically distinct deformation patterns trigger divergent molecular responses, with the sharp nanoneedles upregulating nuclear lamin A (LMNA) expression while simultaneously reducing the nuclear translocation of yes-associated protein (YAP). This mechanosensitive transcriptional coactivator regulates growth-promoting genes. These findings directly link the high-aspect-ratio nanostructure geometry, nuclear mechanics, and transcriptional regulation, demonstrating how physical parameters can be manipulated to control cell fate decisions.

Complementary studies by Li et al. revealed that U2OS cells cultured on quartz nanopillars exhibited reduced YAP nuclear localization and diminished formation of large FAs ($>1\ \mu m^2$) [125]. In this regard, mechanistic investigations implicated clathrin-mediated endocytosis in the removal of integrin $\beta 1$ from the cell surface. This process leads to FA disassembly and altered mechanotransduction signaling, highlighting the intricate relationship between membrane-trafficking and mechanical sensing.

The nuclear envelope functions as a critical mechanosensitive structure that actively participates in vertically aligned nanostructure-mediated signaling through specialized molecular connectors. Lestrell et al.. demonstrated that nuclear deformation in response to vertical nanostructures is precisely regulated by the linker of nucleoskeleton and cytoskeleton (LINC) complex, a transmembrane protein assembly that physically bridges the cytoskeleton and nucleoskeleton [15]. Their studies revealed that the enhanced nuclear deformation mediated by the LINC complex directly correlated with increased cell migration velocity, establishing nuclear mechanotransduction as a key regulator of cellular motility.

This mechanistic insight has enabled innovative applications. For example, Zeng et al. developed quartz nanopillar arrays capable of distinguishing cancer cells from their benign counterparts on the basis of lamin A-dependent variations in nuclear deformation and corresponding migration patterns [17]. Similarly, Tai et al. demonstrated that engineered nanotopographies can effectively recapitulate different stages of cancer progression and visualize metastatic transformation processes [95]. These platforms offer dual utility for screening potential therapeutic candidates and elucidating the molecular mechanisms underlying drug responses, potentially facilitating more targeted therapeutic selection. Collectively, these studies illustrate how a mechanistic understanding of cell–nanoneedle interactions can drive transformative applications in both fundamental research and clinical settings.

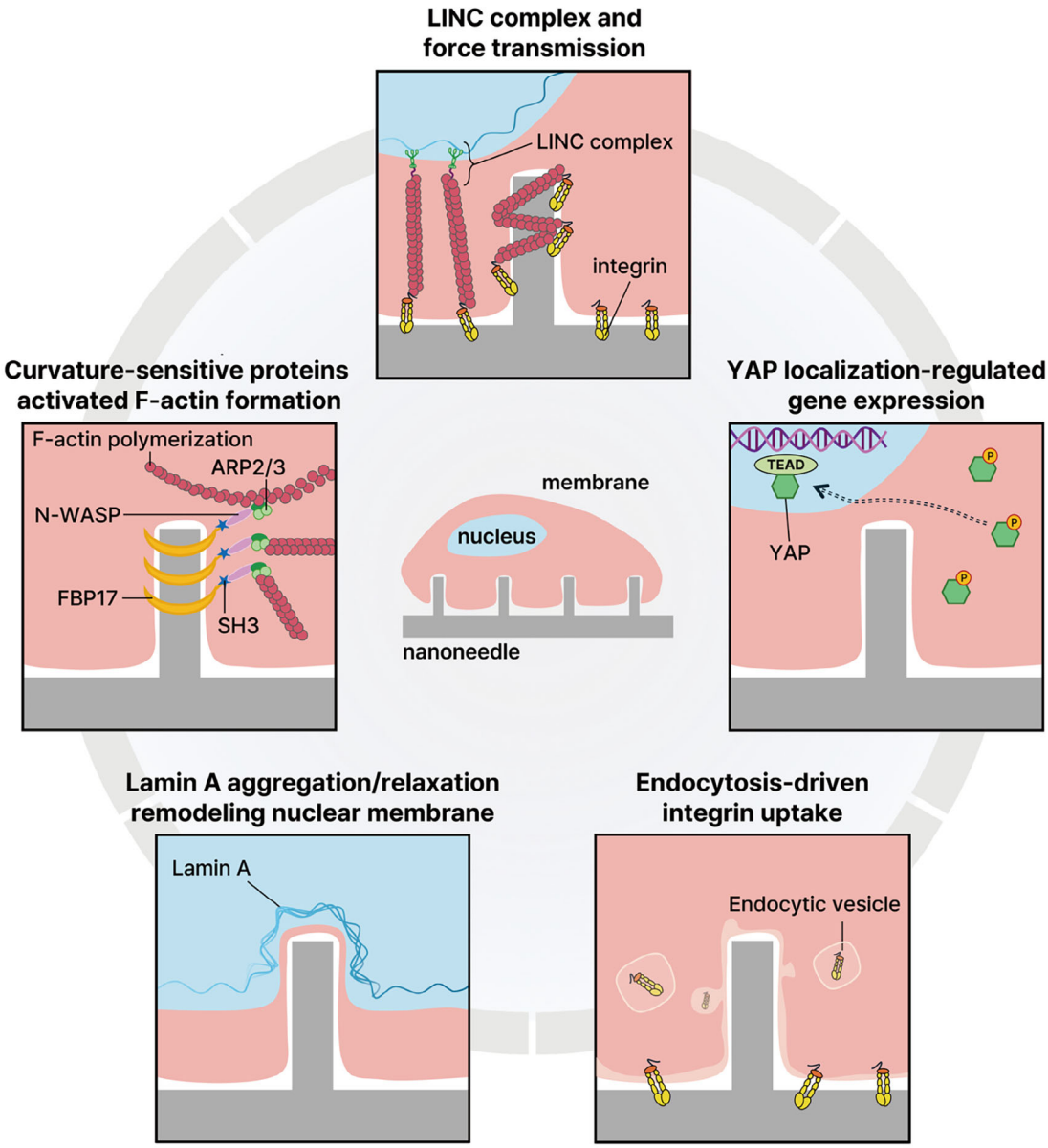

FIGURE 4 | Various mechanotransduction pathways induced by high-aspect-ratio nanostructures.

3.3 | Controlling Cell Phenotypes through Mechanical Programming

Different cell types exhibit distinct preferences for particular mechanical microenvironments, reflecting their native tissue contexts and evolved mechanosensing machineries. This phenomenon, which is termed 'mechanical memory,' originates from cells' adaptation to the stiffness of their physiological tissues: neurons reside in soft brain tissue (~0.1–1 kPa), myocytes in intermediate-stiffness muscle (~8–17 kPa), and osteoblasts in the rigid bone matrix (~25–40 kPa) [126]. Consequently, these cell types have evolved distinct mechanotransduction machineries, including integrin expression profiles, FA composition, and cytoskeletal organization, that are optimized for sensing and responding to their native mechanical environments [99, 100].

At the molecular level, these preferences are mediated by mechanosensitive transcriptional regulators, particularly YAP and transcriptional coactivator with PDZ-binding motif (TAZ). These regulators translocate to the nucleus on stiff substrates to promote proliferative and osteogenic gene programs while remaining in the cytoplasm on soft substrates to favor adipogenic or neurogenic differentiation [127–129]. Complementary pathways involve lamin A, a nuclear envelope protein whose expression increases with substrate stiffness, reinforcing nuclear mechanics and modulating chromatin accessibility for lineage-specific gene expression [130, 131]. The FA size and maturation state further dictate mechanical signal amplification, with large, mature FAs ($>1\ \mu m^2$) forming preferentially on stiff substrates and transmitting stronger contractile forces that activate osteogenic programs, while small, transient FAs on soft substrates favor neural specification. These molecular insights have guided the rational design of nanostructure platforms for directed differentiation. Park et al. developed a flexible patch-type nanoneedle scaffold capable of guiding the differentiation of dental pulp stem cells (DPSCs) through precise spatial control of needle arrangements (Figure 5a) [18]. Their mechanistic investigations revealed that

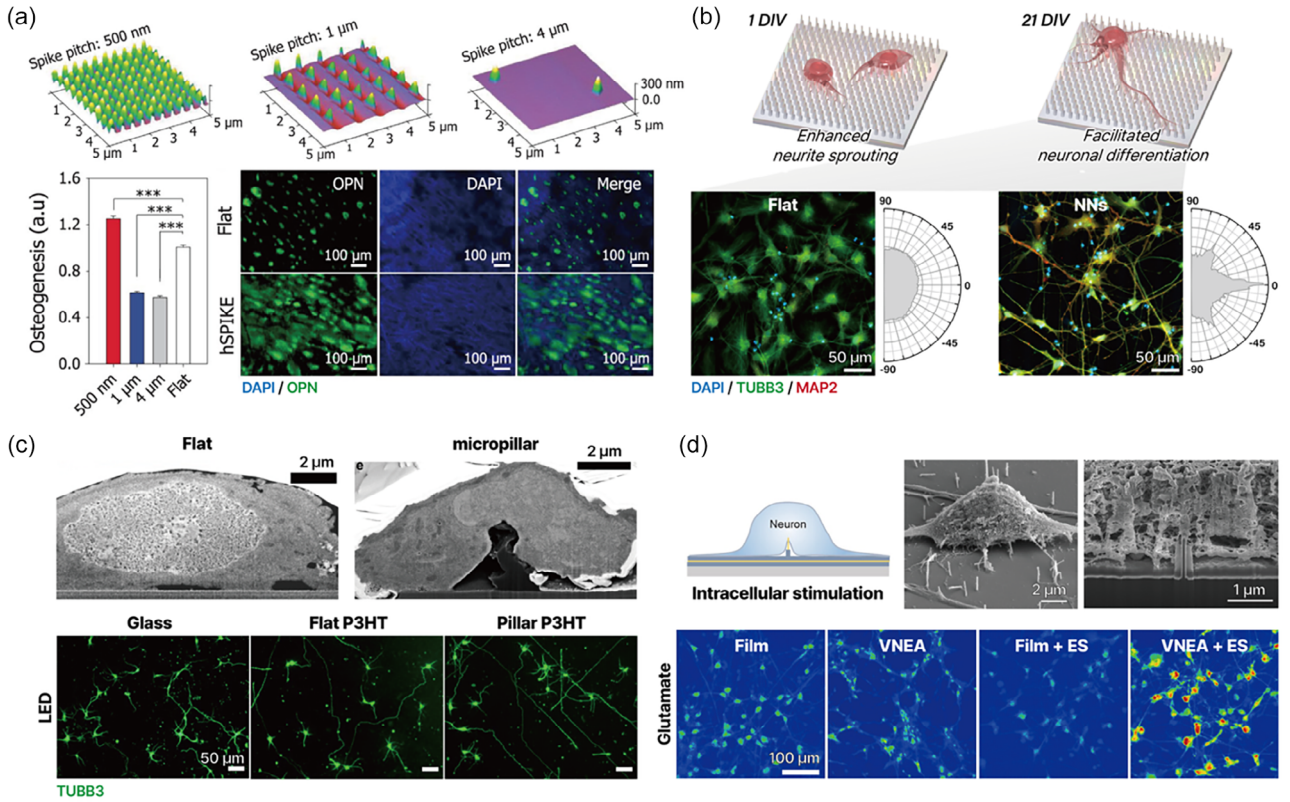

FIGURE 5 | Cell differentiation induced by vertically aligned high-aspect-ratio nanostructures from various studies. (a) The 500 nm-pitch hydrogel nanospike array (hSPIKEs) enhances osteogenesis of DPSCs, as indicated by the increased fluorescence intensity of the osteogenic marker osteopontin (OPN). Reproduced with permission [18]. Copyright 2019, American Chemical Society. (b) Neuronal maturation of NPCs is enhanced on PUA nanoneedles after 21 days of differentiation. Reproduced with permission [45]. Copyright 2025, Nature Springer. (c) Neuronal growth of primary neurons is enhanced on photostimulated P3HT micropillars. Reproduced with permission [89]. Copyright 2021, American Chemical Society. (d) Differentiation of human fetal neural stem cells (hfNSCs) to functional neuronal cells is promoted by intracellular stimulation on VNEA. Reproduced with permission [32]. Copyright 2021, American Chemical Society.

the nanoneedle tips created localized mechanical stimuli that enhanced the secretion of osteogenic growth factors through a signaling cascade involving FA remodeling, cytoskeletal reorganization, YAP nuclear translocation, and lamin A redistribution [116]. This mechanotransduction pathway ultimately established an osteogenic transcriptional program, demonstrating how purely physical cues can initiate complex differentiation processes. Similarly, hierarchical nanostructures combining nanopillars with microwrinkles and biomimetic architectures designed to recapitulate the native ECM of cardiac tissues have been shown to promote the maturation of cardiomyocytes with improved functional characteristics [132].

Material stiffness is a critical parameter in nanostructure-mediated differentiation, with different cell types exhibiting distinct preferences for specific mechanical microenvironments [47]. Remarkably, cells cultured on nanostructured substrates show an apparent reduction in stiffness in comparison with those cultured on flat surfaces of identical material composition, with measurements showing a 46% reduction in the perceived rigidity to levels comparable to 1-kPa hydrogels [125]. This phenomenon effectively creates mechanically 'softer' niches even when using relatively rigid materials, significantly expanding the versatility of vertical nanostructure platforms for cell types that preferentially thrive in compliant environments, particularly cells of neural lineages.

Yang et al. exploited this principle by fabricating pillar arrays using soft PUA to investigate neural differentiation dynamics [102]. Their systematic analysis revealed that higher-density nanopillars with reduced intercellular spacing significantly enhanced both neuronal and glial differentiation, as evidenced by the upregulation of lineage-specific markers, including the neuronal marker beta-tubulin III (TUBB3) and the astrocytic marker glial fibrillary acidic protein (GFAP). The neural-promoting effects of soft nanotopographies were further confirmed by Jang et al., who demonstrated that neural progenitor cells (NPCs) cultured on PUA nanoneedle arrays exhibited enhanced neuronal differentiation and improved cell alignment, as confirmed by the improved fluorescence intensity of TUBB3 and microtubule-associated protein 2 (MAP2) (Figure 5b) [45]. In comparative analyses, NPCs cultured on PUA nanoneedles showed significantly higher expression of neuronal markers than NPCs cultured on silicon counterparts with identical geometry and a substantially higher Young's modulus, highlighting the critical importance of mechanical properties in determining differentiation outcomes.

Beyond passive topographical guidance, emerging combinatorial approaches that integrate vertical nanostructures with complementary stimuli have yielded synergistic platforms with enhanced capabilities for directing cellular differentiation. Among these approaches, electroactive engineering has

demonstrated promise for promoting neuronal differentiation and functional network formation [133]. Milos et al.. developed poly(3-hexylthiophene-2,5-diyl) (P3HT) micropillar arrays with intrinsic optoelectronic properties, leveraging the structural characteristics of nanostructures to establish intimate contact with neuronal membranes (Figure 5c) [89]. Upon visible-light illumination, these photosensitive nanostructure arrays generated localized electrical stimuli that enhanced neurite extension and guided alignment along predefined topographical patterns.

Complementary work by Kwon et al. has demonstrated that a vertical nanowire electrode array (VNEA) can facilitate direct intracellular electrical stimulation by delivering a localized electrical current through stable membrane-penetrating interfaces (Figure 5d) [32]. These integrated approaches effectively combine the topographical guidance provided by the nanowire architecture with electromagnetic stimuli that mimic physiological signaling, creating biomimetic microenvironments that promote enhanced neuronal maturation and network formation. Such platforms offer unprecedented opportunities for in vitro neural development and circuit formation, yielding more physiologically relevant drug-screening platforms and advanced neural tissue engineering applications.

Although electrical stimulation has been extensively employed to enhance nanostructure-mediated differentiation, similar integrated approaches combining mechanical, electrical, and biochemical cues have also been developed for advanced intracellular delivery systems [7, 34, 134]. These multifunctional platforms represent the next frontier in nanoneedle technology, wherein the fundamental understanding gained from classical mechanotransduction studies is being translated into advanced therapeutics and diagnostics. The following chapter explores these emerging frontiers, focusing on recent advances in nanostructure-based delivery systems and their integration with complementary stimuli to enhance therapeutic outcomes across diverse biomedical applications.

4 | High-Aspect-Ratio Nanostructures for Precision Medicine

The translation of high-aspect-ratio nanostructure platforms from fundamental research tools to clinical therapeutics is one of the most promising developments in nanomedicine [135]. These sophisticated structures can address critical challenges in drug delivery and targeted therapy by providing direct access to intracellular compartments and enabling precise tissue-level interventions. This section explores the evolution of nanostructure technologies across two complementary domains: cellular-level delivery systems that overcome membrane barriers for intracellular targeting (Section 4.1) and in vivo applications that enable localized therapeutic interventions in complex tissues (Section 4.2). To facilitate comparisons across different therapeutic-delivery approaches, Table 3 summarizes the key characteristics of representative delivery methods, including conventional systemic routes and micro-/nanoneedle-based strategies, with respect to targeting capability, invasiveness, and translational potential.

TABLE 3 | Comparison of therapeutic delivery methods, including micro- and nanoneedle-based platforms.

Delivery method	Delivery efficiency	Cytotoxicity	Cargo flexibility	Localized control	Scalability	Ref
Liposomes	Variable	High	Limited for macromolecular biologics	Nonlocalized	High	[136]
Viral vector	Variable	Amount-dependent	Depending on vector type	Non-localized	Low	[137]
Conventional electroporation	Bulk delivery	Significant cellular damage	Broad	Limited spatial control	Moderate	[138]
High-aspect-ratio nanostructure	Direct physical access	Minimal cellular damage	Diverse therapeutic payloads	Precise tissue-level interventions	Device-integrated	[25, 139]

4.1 | Intracellular Access: Vertical Nanostructure-Mediated Delivery Systems

The plasma membrane is a formidable barrier to therapeutic delivery, particularly for macromolecular biologics and nucleic acid-based medicines. In this regard, high-aspect-ratio nanostructure platforms have emerged as revolutionary tools for overcoming delivery challenges by providing direct physical access to the cell interior while preserving cellular viability. Their structural adaptability, customizable surface properties, and precisely tunable mechanical characteristics enable controlled penetration into cells while minimizing cellular damage, facilitating localized delivery of diverse therapeutic payloads. Upon cellular engagement, therapeutic agents can be delivered through multiple mechanisms: encapsulation within the structure [71], adsorption onto functionalized surfaces [21, 22, 24], or active fusion through engineered channels [7, 34, 70, 140].

The design of nanostructure delivery systems has evolved in parallel with the increasing complexity of therapeutic cargoes from small molecules (e.g., drugs [20, 141], fluorescent dyes [34, 62], quantum dots [72], and nanoparticles [142]) to large biomolecules (e.g., proteins [71, 143], enzymes [7, 23], and nucleic acids [6, 21, 43, 134]). This evolution has driven the development of diverse structural architectures and material compositions that are tailored to specific delivery requirements. The following sections examine key innovations in nanostructure design for intracellular delivery, highlighting structural variations, advanced functionalization strategies, and synergistic approaches that can enhance therapeutic efficacy.

4.1.1 | Architectural Diversity in High-Aspect Ratio Nanostructure Design

4.1.1.1 | Solid Nanostructure Platforms: Leveraging Mechanical Penetration and Endocytosis. Solid high-aspect-ratio structures, which utilize mechanical penetration to bypass the plasma membrane and initiate localized endocytosis at the cell–structure interface, are widely employed for intracellular delivery. When these structures engage with cellular membranes, they induce curvature-dependent deformation and FA formation, activating endocytic pathways that facilitate cargo internalization (Figure 6a) [47]. Various materials have been explored for fabricating solid nanostructures, including stainless steel [144], nickel [145], silicon [6, 22, 23], quartz [17, 125], and polymers [8, 9, 47], with each offering distinct advantages for specific applications.

Metallic nanostructures provide exceptional mechanical strength, enabling reliable penetration of dense tissues [73]. However, their clinical translation has been constrained by potential biocompatibility concerns, particularly for nickel-based structures [74], along with their relatively high production costs and fabrication complexity. Among the metallic materials, Au has gained particular interest owing to its excellent biocompatibility and established use in microelectrode arrays (MEAs) for electrophysiological applications [75, 76]. In addition to their sensing capabilities, vertical Au nanostructures have demonstrated substantial potential for controlled therapeutic delivery, as exemplified by Kavaldzhiev et al., who developed Au microneedles capable of localized heating for controlled drug release [77]. More recently, silicon [78–80] and polymer-based [47] vertical needle arrays have been engineered to enhance intracellular transport while providing improved mechanical compliance and biocompatibility for sensitive cellular applications.

4.1.1.2 | Hollow Nanostructure Systems: Enabling Direct Fluidic Delivery. Although solid nanostructures can effectively facilitate endocytosis-mediated cargo uptake, hollow architectures offer complementary advantages by functioning as direct conduits for fluidic cargo delivery. These sophisticated structures feature an internal channel that enables precise infusion of therapeutic agents directly into the intracellular environment (Figure 6b) [38]. The hollow core serves as a protective pathway for therapeutic solutions, which can be delivered through various mechanisms, including passive diffusion [53], capillary action [146], or pressure-driven flow [147]. This architectural design can enable unprecedented control over dosage and release kinetics, making hollow nanostructures particularly valuable for applications requiring sustained therapeutic effects or precise temporal control of delivery [148].

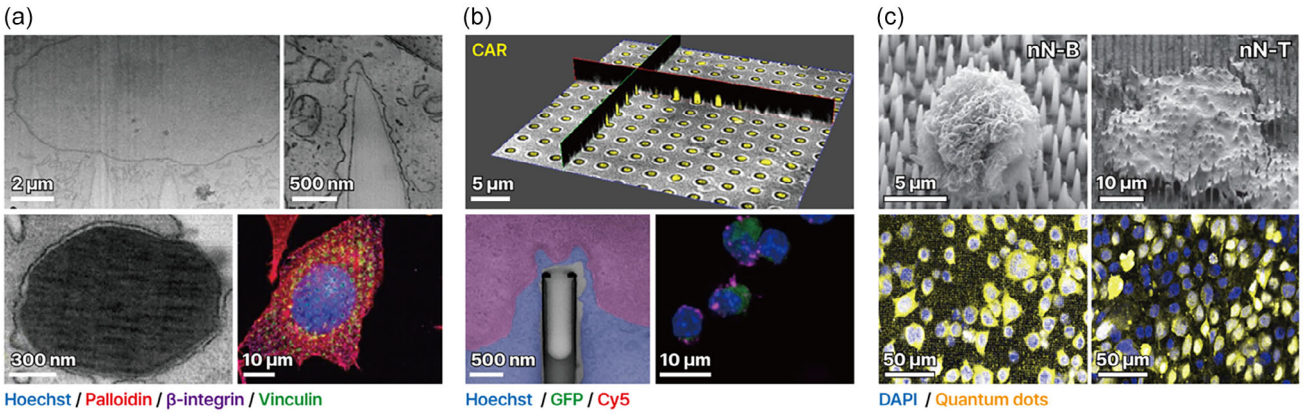

FIGURE 6 | Structural variations of high-aspect ratio nanostructure arrays utilized in drug delivery. (a) Solid-type polystyrene nanoneedles induce membrane deformation in GPE86 cells, which activates endocytosis. Reproduced with permission [47]. Copyright 2021, Wiley. (b) Hollow silicon nanotubes effectively deliver Cy3-tagged chimeric antigen receptor (CAR) constructs to T cells. Reproduced with permission [38]. Copyright 2023, Elsevier Ltd. (c) Porous silicon nanoneedles allow rapid cytosolic delivery and preserve HeLa cell morphology following nanoinjection. Reproduced with permission [72]. Copyright 2015, American Chemical Society.

4.1.1.3 | Porous Nanostructures: Maximizing Cargo Capacity and Release Kinetics. Porous nanostructure designs represent a sophisticated approach that leverages high surface areas and interconnected void spaces to enhance both the cargo-loading capacity and delivery efficiency. Chiappini et al. demonstrated the remarkable potential of porous silicon nanoneedles with precisely controlled 10–15 nm diameter pores, which allowed efficient intracellular delivery of 6 nm quantum dots (Figure 6c) [72]. Their systematic investigation compared two distinct delivery configurations: nanoneedles-on-bottom (nN-B) versus nanoneedles-on-top (nN-T). Notably, the nN-T configuration significantly accelerated the delivery rate, achieving deeper interfacial penetration within 1 min, which was comparable to the profile observed with the nN-B configuration after 8 h. These findings highlight the extraordinary potential of porous nanoneedles for rapid and efficient therapeutic delivery, with implications for clinical applications that require precise temporal control of drug release.

4.1.2 | Advanced Strategies for Enhanced Therapeutic Delivery

Although passive diffusion and simple mechanical penetration can effectively deliver small molecules, delivery of macromolecular therapeutics often requires additional strategies to overcome the size- and charge-related barriers to intracellular transport. To address this challenge, researchers have developed various collaborative approaches that combine vertical nanostructure platforms with complementary technologies, including electroporation [6, 7, 140], mechanical stimulation [23, 149], and surface functionalization [21, 22, 24]. These strategies can significantly enhance the delivery efficiency of complex therapeutics while maintaining high cell viability, making them highly promising for clinical translation.

4.1.2.1 | Electroporation-Enhanced Nanostructure Systems: Synergistic Membrane Disruption. Electroporation is a well-established technique that employs electrical pulses to temporarily disrupt membrane integrity and thereby enhance intracellular drug delivery. When integrated with nanostructured platforms, this approach uses highly localized electrical fields that create transient membrane openings with minimal cell damage. Importantly, vertically aligned nanostructures perform dual functions in this context: they physically stabilize cells during electroporation and extend the membrane resealing time, allowing enhanced cargo entry while reducing the voltage requirements in comparison with conventional electroporation methods.

Liu et al. developed an integrated silicon-nanoneedle electroporation system powered by a triboelectric nanogenerator (TENG) [6]. In this platform, nanoneedles served as both electrodes and physical stabilizers, ensuring precisely controlled membrane disruption and enhanced therapeutic entry. This system achieved remarkable outcomes, showing 82% siRNA delivery efficiency while maintaining 94% cell viability and performance metrics that substantially exceeded those of conventional transfection methods. In a complementary investigation, Liu et al.. engineered a hollow nanoneedle array (HNA)-electroporation platform designed for delivery of Cas9/sgRNA ribonucleoprotein (RNP) complexes directly in the nucleus (Figure 7a) [7]. The strategic positioning of nanoneedles, which bridged the plasma membrane and nuclear envelope, enabled highly efficient gene editing with minimal electrical input, demonstrating the potential of this method for precisely targeted genomic modifications.

The integration of electroporation with nanostructured platforms offers major advantages over conventional electroporation approaches, most notably the substantial reduction in the required voltage [138]. This reduction minimizes cellular damage and facilitates the intracellular transport of macromolecular proteins [25, 139], establishing nanoneedle-based electroporation as a promising platform for transferring complex biologics with high precision and reduced cytotoxicity.

4.1.2.2 | Vibration-Assisted Delivery: Mechanical Enhancement of Membrane Permeability. In addition to electroporation, mechanical stimulation strategies have also been developed to enhance vertical nanostructure-mediated delivery without chemical or electrical intervention [149]. Li et al.. introduced a vibration-assisted nanoneedle/microfluidic system that achieved efficient delivery of Cas9/RNP complexes solely through controlled mechanical forces (Figure 7b) [23]. This strategy minimized cellular stress while creating optimally sized membrane pores for macromolecular transport, offering a minimally invasive alternative to conventional transfection methods for sensitive cell types and clinical applications.

4.1.2.3 | Surface-Engineered Nanostructures: Stimuli-Responsive Therapeutic Release. Surface functionalization is a strategy for enhancing the loading capacity, targeting specificity, and controlled release of therapeutics from nanostructured platforms. By incorporating stimuli-responsive elements, researchers have developed 'smart' vertical nanostructures that respond to the intracellular environment, ensuring precise temporal and spatial control over therapeutic release while minimizing off-target effects.

Redox-responsive surface modifications are another promising approach for controlled intracellular delivery. Liu et al. functionalized silicon nanowires with polyethylenimine (PEI) linked to N, N′-cystamine-bis-acrylamide (CBA), a biodegradable cationic polymer containing disulfide bonds [22]. After cellular internalization, elevated cytoplasmic glutathione (GSH) levels trigger disulfide bond cleavage, leading to the controlled release of DNA cargo. This environment-specific release mechanism significantly enhanced intracellular gene delivery while reducing the cytotoxicity typically associated with conventional PEI delivery systems [150, 151]. Expanding on this concept, Hachim et al. employed layer-by-layer (LbL) self-assembly to create ultrathin polymer coatings on nanoneedles (Figure 7c) [21]. Their comparative analysis revealed that surface-modified nanostructures significantly outperformed their unmodified counterparts in terms of plasmid DNA and delivery efficiency.

pH-responsive systems take advantage of the intrinsic pH gradients across the extracellular space, endo/lysosomal compartments, and pathological tissues such as tumors or inflamed regions [152]. For example, porous polymer–coated microneedles incorporating acid-sensitive components have been shown to remain stable under physiological pH conditions while undergoing rapid structural disruption and drug release in acidic microenvironments [153]. This selective activation enhances the therapeutic index by concentrating drug release at disease sites while minimizing systemic exposure.

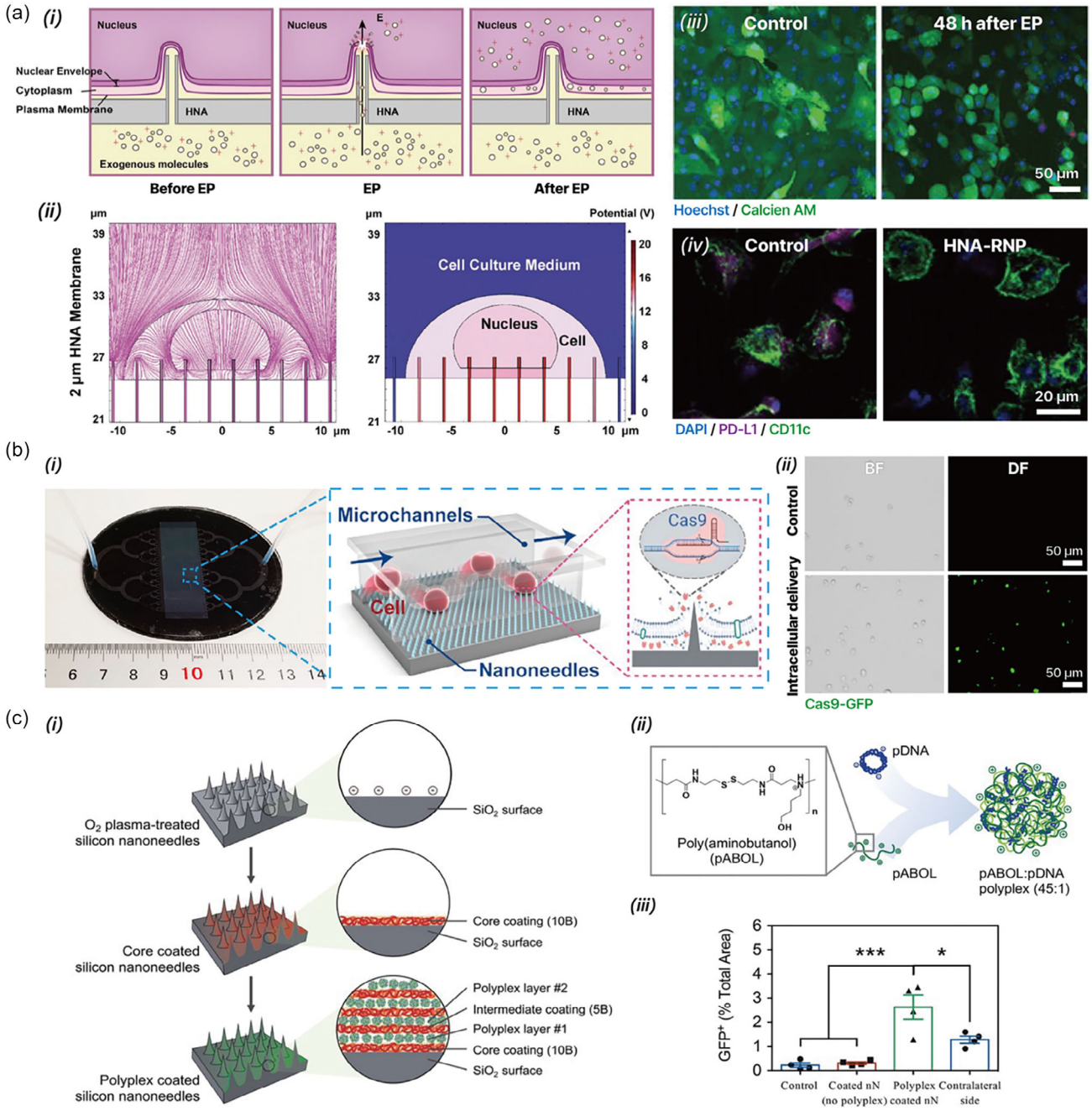

FIGURE 7 | Various approaches combining nanostructure platforms with complementary technologies. (a) (i) Schematic illustration of intranuclear molecular delivery via the HNA combined with electrical poration (EP). (ii) Electric potential and electric field distribution in the presence of HNA revealed strong electric field aggregation at the HNA tips interacting with cells. (iii) Live/dead staining of bone marrow-derived dendritic cells (BMDCs) showed >98% viability. (iv) Significant Programmed death ligand 1 (PD-L1) downregulation was observed only in Cas9/sgRNA-delivered groups, confirming effective knockout. Reproduced with permission [7]. Copyright 2024, Wiley. (b) (i) Photograph and schematic design of vibration-assisted nanoneedle/microfluidic platform for intracellular delivery. (ii) Bright field (BF) and dark field (DF) images of NK-92 cells before and after intracellular delivery of Cas9/GFP RNPs. Reproduced with permission [23]. Copyright 2022, American Chemical Society. (c) (i) Schematic of the polysaccharide-polyplex nanofilm coating procedure on silicon nanoneedles using an LbL assembly. (ii) Polyplex formation between pDNA and pABOL in a mass ratio 1:45. (iii) Quantification of GFP expression based on image analysis, indicating enhanced transfection efficiency in the nanoneedle group coated with 4-polyplex nanofilms compared to the control group. Reproduced with permission [21]. Copyright 2022, Wiley.

Enzyme-responsive nanoneedle platforms can further refine biological selectivity by exploiting disease- or tissue-associated enzymatic activities. Functionalization with enzyme-cleavable peptides or prodrug motifs can enable nanostructures to undergo controlled activation or degradation in response to local enzymatic cues, allowing site-specific therapeutic release while minimizing off-target effects. For example, enzyme-responsive peptide–prodrug–integrated microneedle patches have been developed to achieve efficient transdermal delivery, wherein esterase-mediated cleavage selectively activates the therapeutic payload and significantly enhances in vivo efficacy in comparison with conventional oral administration [154].

In contrast to endogenous stimuli, light-responsive nanoneedle-based delivery strategies enable externally programmable control over therapeutic activation with high spatial and temporal precision. By integrating photoresponsive or photothermal components, these systems allow on-demand drug release upon light irradiation. Hybrid hydrogel-based transdermal patches incorporating photothermal nanoparticles have demonstrated visible-light-triggered volume changes that enable localized and on-demand drug release, illustrating the potential of optical control for precise transdermal delivery [155]. Milos et al. developed poly(3-hexylthiophene) (P3HT) micropillar arrays with intrinsic photosensitivity, and visible-light illumination generated localized electrical stimuli that enhanced neurite extension and guided neuronal alignment [89].

Collectively, these diverse stimulus-responsive strategies allow environment-specific or on-demand therapeutic activation, thereby expanding the functional versatility of nanoneedle-based delivery systems across diverse biomedical applications. The selection of an appropriate triggering mechanism depends on disease-specific characteristics (pH, enzyme expression, and temperature), accessibility to external stimuli (light and magnetic fields), and desired release kinetics (sustained vs. pulsatile). In this regard, combinations of multiple stimuli, such as pH-responsive polymers with redox-sensitive linkers, are being increasingly explored to achieve sequential, multistage release profiles that mimic complex biological processes and optimize therapeutic outcomes.

4.2 | Translating High-Aspect-Ratio Nanostructure Technologies to In Vivo Applications

Although in vitro delivery systems have established the fundamental capabilities of nanostructured platforms, translation of these platforms to in vivo applications represents a critical milestone in clinical implementation. As discussed in Section 2.4, material selection for in vivo applications depends critically on balancing mechanical performance, biocompatibility, degradation behavior, and manufacturing scalability. Silicon and biodegradable polymers have emerged as the two most clinically advanced platforms—silicon offers nanoscale precision and controlled degradation and polymers provide FDA-approved biocompatibility and scalable manufacturing—making them the primary focus of current translational efforts.

This section examines the recent advances in translating nanostructure technologies into in vivo applications. These advances are organized by disease categories to highlight their clinical potential across diverse medical contexts. Each subsection integrates examples from both silicon and polymeric platforms, explicitly noting how material selection responds to application-specific requirements.

Beyond structural and material design, nanostructure-mediated delivery fundamentally alters drug pharmacokinetics and bioavailability in comparison with conventional routes. By bypassing biological barriers, including the stratum corneum for transdermal delivery and first-pass hepatic metabolism for systemic therapeutics, these platforms can achieve superior bioavailability with reduced interpatient variability [156]. The controlled degradation kinetics and matrix-mediated diffusion afforded by these systems can enable sustained therapeutic release, extending dosing intervals from hours to weeks or months while maintaining plasma concentrations within therapeutic windows. For tissue-targeted applications, localized delivery can achieve high local drug concentrations while minimizing systemic exposure and off-target toxicity and is particularly valuable for therapeutics with narrow therapeutic indices. These pharmacokinetic advantages—enhanced bioavailability, sustained release, reduced variability, and localized delivery—translate directly into improved patient compliance, predictable therapeutic responses, and enhanced safety profiles, as demonstrated in the disease-specific applications discussed below.

4.2.1 | Ocular Diseases and Vision-Threatening Conditions

Ocular drug delivery presents unique challenges owing to anatomical barriers, including the cornea, the blood-retinal barrier, and rapid tear turnover, which limit therapeutic bioavailability. High-aspect-ratio nanostructures have emerged as promising platforms for sustained intraocular drug delivery with minimal invasiveness.

A primary concern regarding the use of silicon-based high-aspect-ratio nanostructures is their long-term biocompatibility with living tissues. To address this challenge, researchers have developed biodegradable silicon nanostructures with high aspect ratios using precisely engineered porous architectures [72]. These nanoneedles facilitate efficient nanoparticle delivery and undergo controlled degradation in physiological environments, thereby eliminating the need for surgical retrieval and reducing the risk of chronic foreign body reactions [19]. Despite these advances, the inherent rigidity and brittleness of silicon nanostructures present ongoing challenges for in vivo applications, particularly in terms of the risk of mechanical failure during tissue penetration. In addition, the optical opacity of silicon limits its utility in applications that require real-time imaging or light-controlled therapeutic release. To overcome these limitations, researchers have developed alternative strategies that can enhance the adaptability of these nanostructures to biological tissues while maintaining their controlled release profiles.

Various transfer techniques have been developed to seamlessly integrate silicon-based vertical nanostructures onto soft, biocompatible substrates, enhancing their mechanical compliance, optical transparency, and conformability to complex tissue geometries. Kim et al. pioneered this approach by fabricating silicon nanoneedles on PDMS substrates and leveraging the controlled swelling properties of this elastomer [62]. By introducing strategic undercuts through potassium hydroxide etching, they successfully transferred nanostructure arrays onto flexible substrates. This method enabled the uniform distribution of nanoneedles across curved PDMS surfaces, significantly enhancing the efficacy for transdermal therapeutic delivery.

Park et al. further expanded this concept by integrating silicon nanoneedles into polyvinyl alcohol (PVA) contact lenses for sustained ocular drug delivery over several months [20]. The biodegradability of the substrate and nanoneedles eliminated the need for surgical removal, whereas the biphasic release profile (initial burst followed by sustained diffusion over 55 days) provided

continuous therapeutic levels without the plasma concentration fluctuations associated with repeated intravitreal injections.

Wang et al. proposed the integration of silicon nanoneedles into diverse medical devices, including hydrogels, catheter tubes, and contact lenses, for efficient nucleic acid delivery to cells and tissues (Figure 8) [43]. Their investigation employed three distinct etching methods, MACE, RIE, and ECE, to precisely control the nanostructure dimensions and surface porosity. Notably, by reducing the thickness of the support layers to nearly 0 nm after transfer, these nanoneedles achieved a significantly higher transfection efficiency than conventional lipofectamine-mediated delivery systems. When incorporated into a commercial bandage, these nanoneedles adhered securely to the skin and adapted to its dynamic movements. This facilitated uniform nucleic acid delivery across curved skin regions in a live mouse model.

These platforms address critical unmet needs in ophthalmology, where patient compliance with frequent intravitreal injections (often monthly) remains challenging. By extending dosing intervals to 3–6 months through sustained-release kinetics and achieving bioavailability comparable to that of direct injection while eliminating the administration burden, sustained-release nanostructure systems could potentially extend dosing intervals to 3–6 months, dramatically improving treatment adherence and patient quality of life.

4.2.2 | Wound Healing and Tissue Regeneration

Chronic wounds, particularly in patients with diabetes, represent a major healthcare burden affecting >6.5 million patients in the US alone. Polymeric high-aspect-ratio microstructures have shown promise in addressing complex wound-healing challenges through multifunctional therapeutic delivery. Polymeric structures offer tunable mechanical properties, enhanced biocompatibility, and controlled biodegradability, enabling minimally invasive and precise regulation of drug administration [157]. Although typically limited to microscale dimensions, the carefully engineered designs of these structures ensure minimal discomfort and tissue disruption while maintaining effective therapeutic delivery.

The mechanical properties of polymeric microstructures represent a critical design consideration, since these structures must possess sufficient strength to penetrate biological barriers while maintaining their biodegradability and flexibility. For successful skin penetration without structural failure, high-aspect-ratio polymeric microstructures generally require a minimum

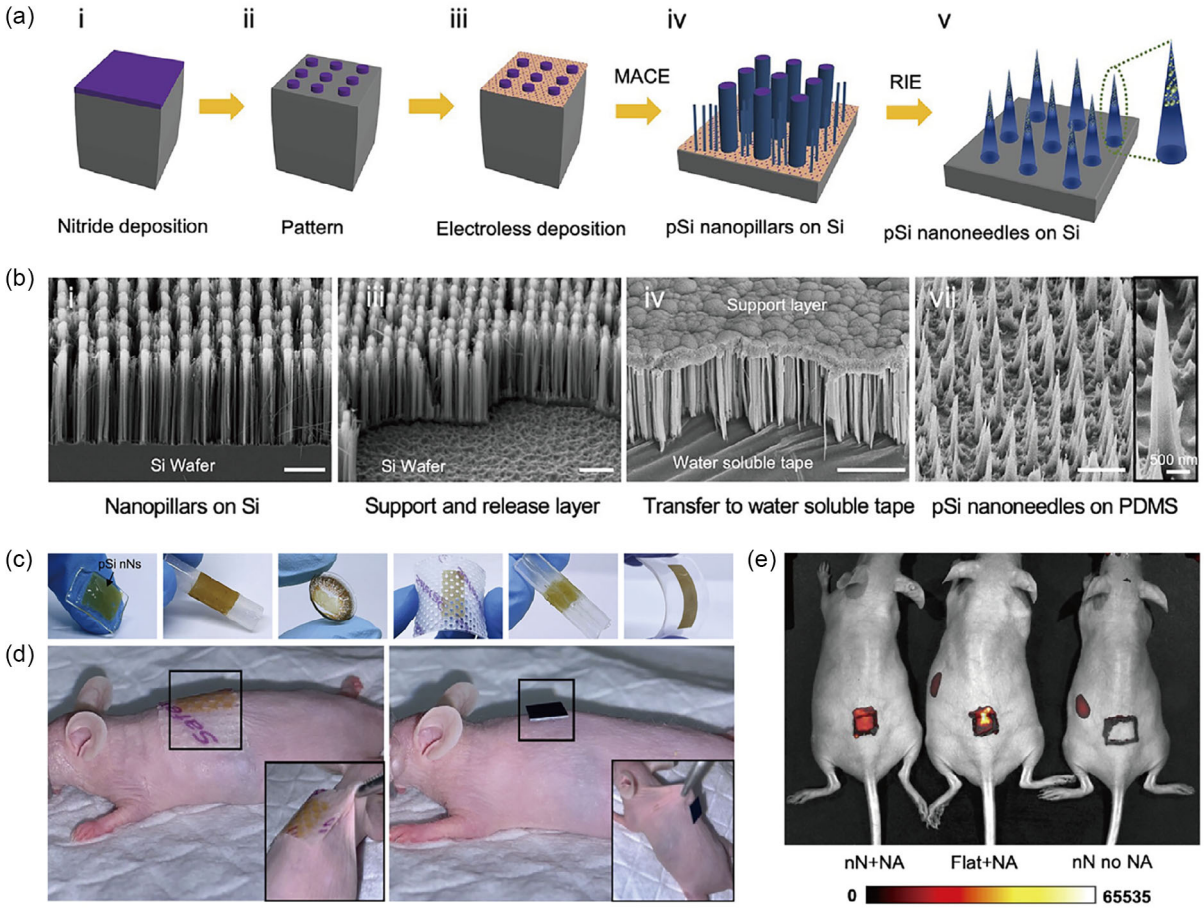

FIGURE 8 | Various silicon nanostructure platforms integrated into flexible and transparent substrates for in vivo applications. (a) Schematic of the porous silicon (pSi) nanoneedle fabrication process. (b) SEM images showing the process of nanoneedle transfer on PDMS. (c) Various silicon nanoneedles are integrated with medical devices, such as biodegradable gelatin, hydrogel contact lenses, wound bandages, sharp, convex structures, and PLA film (from left to right). (d) Images of a nanoneedle-integrated bandage conforming to mouse skin for in vivo nanoinjection, in contrast to a rigid chip detaching under skin motion. (e) Near-infrared live imaging revealed uniform and enhanced delivery of fluorescently labeled plasmid through nanoneedles integrated in a flexible patch. Reproduced with permission [43]. Copyright 2024, American Chemical Society.

mechanical strength of approximately 0.1 N per structure [11], a threshold that guides material selection and structural engineering.

Zhang et al. developed core–shell microneedles featuring a PVA outer shell loaded with verteporfin (VP) and an inner core of cross-linked heparin (Figure 9) [9]. When applied to wound sites, these multifunctional structures simultaneously inhibited bacterial biofilm formation while releasing VP to block Engrailed-1 (*En1*) activation. Additionally, the cytokines released from infiltrating macrophages interacted with the exposed heparin core, neutralizing inflammatory mediators and facilitating the transition from the inflammatory phase to the proliferative healing phase. In vivo studies using bacteria-infected diabetic mouse models demonstrated significantly accelerated wound healing, confirming the therapeutic efficacy of these bioresponsive microneedle systems.

Nature-inspired designs have increasingly shaped the development of advanced microstructures. Zhu et al.. created a microneedle patch inspired by the blue-ringed octopus, which was specifically designed to adhere to target tissues, penetrate biological barriers, and deliver therapeutic agents with temporal precision [8]. This patch incorporated thermosensitive PNIPAm for temperature-responsive drug release, which was surrounded by tannic acid-functionalized suction cups that provided robust adhesion to the mucosal surfaces. Evaluation of this patch in a mouse melanoma model demonstrated sustained tumor suppression through localized drug administration, highlighting the potential of biomimetic approaches to enhance therapeutic outcomes.

Using a similar biomimetic strategy, researchers developed heparin-based hydrogel-embedded polycaprolactone (PCL) vertical microstructures inspired by coral reef architectures [53]. Upon insertion into the wound site, the hydrogel matrix selectively adsorbed inflammatory proteins while undergoing pH-responsive color changes owing to the incorporated phenol red indicator, transitioning from red in alkaline environments to yellow in acidic conditions. This visual indicator allowed real-time infection monitoring while simultaneously modulating antibiotic-release kinetics, enhancing local drug concentrations in infected (acidic) regions, minimizing systemic absorption, and reducing off-target antibiotic exposure, which is a critical advantage for preventing systemic side effects and antibiotic resistance.

4.2.3 | Cancer Therapy and Tumor Targeting

Conventional cancer therapies face several challenges, including poor tumor penetration, systemic toxicity, and inadequate immune responses. High-aspect-ratio nanostructures enable localized, sustained delivery of therapeutics with reduced systemic exposure. Zhou et al. engineered ice-templated polystyrene microneedles with multiple open grooves to facilitate cellular transport and retention [12]. These microneedles were incorporated into adoptive T cell therapy (ACT) protocols, an immunotherapeutic approach involving the transplantation of T cells engineered to express tumor-specific receptors, including the T cell receptor (TCR) or chimeric antigen receptor (CAR). To further enhance therapeutic efficacy, the microneedles were functionalized with the chemokine CCL22, which selectively recruits regulatory T cells (Tregs), an immunosuppressive cell population, away from the tumor microenvironment. This strategic immunomodulation significantly enhanced antitumor responses in a mouse melanoma model, dramatically extending survival time. Thus, while untreated control animals succumbed to tumor progression within 3 weeks, those receiving microneedle-based immunotherapy survived for up to 7 weeks, demonstrating the remarkable potential of the integrated microneedle platform for advanced cancer treatment. This localized cellular-delivery approach achieved therapeutic cell densities at tumor sites that are unattainable through intravenous infusion, while minimizing the systemic immunosuppression and cytokine release syndrome associated with systemic CAR-T administration.

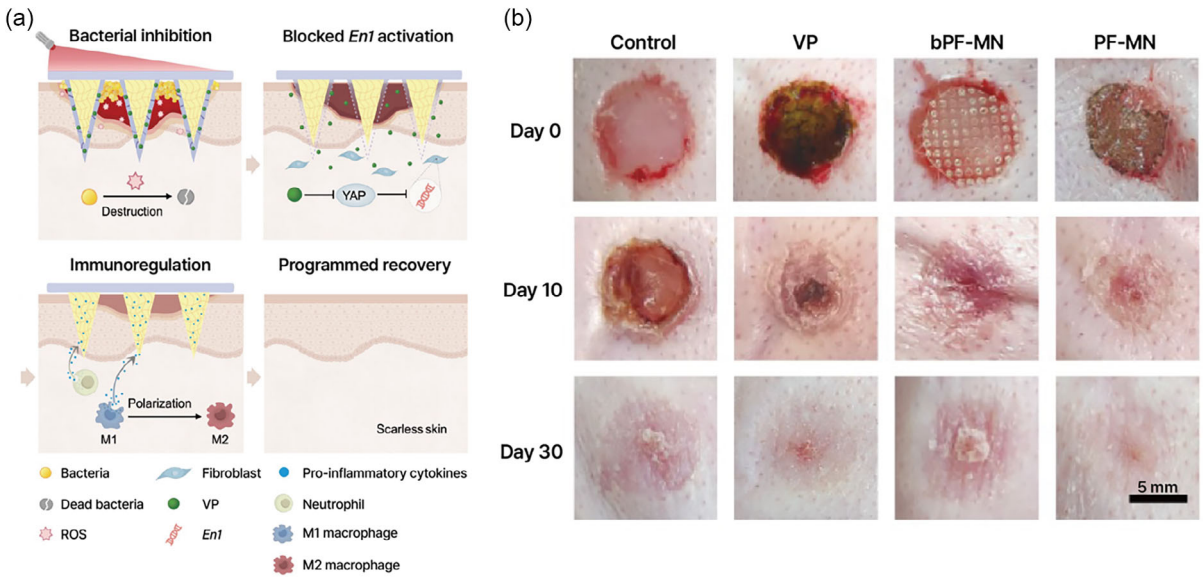

FIGURE 9 | Polymeric microstructures for in vivo applications. (a) Schematic of the programmed-function microneedle (PF-MN) designed for stepwise action: (1) bacterial inhibition, (2) *En1* inactivation, (3) immunoregulation, (4) tissue recovery. (b) Representative photographs of wound sites on rabbit ears after various treatments at designated time points. Both blank PF-MN (bPF-MN) and PF-MN-treated groups exhibited enhanced wound closure. Reproduced with permission [9]. Copyright 2023, Springer Nature.

The convergence of high-aspect-ratio nanostructures and microstructural technologies with advanced therapeutic modalities continues to expand the frontiers of precision medicine. By enabling targeted delivery of diverse therapeutic agents ranging from small molecules and biologics to cellular therapies, these platforms address the fundamental challenges in medical interventions while minimizing off-target effects. As these technologies advance toward clinical implementation, they promise to transform therapeutic approaches across multiple disease domains, offering new possibilities for personalized and minimally invasive treatment strategies.

4.2.4 | Metabolic Disorders and Contraception

Long-acting drug delivery for chronic disease management represents a major opportunity for high-aspect-ratio microstructural platforms, particularly for conditions requiring sustained therapeutic levels. Li et al.. demonstrated the clinical potential of this approach by developing biodegradable microneedles based on PLA and PLGA for transdermal contraceptive delivery [13]. Their design incorporated air-bubble structures that facilitated controlled needle fracture upon insertion, thereby ensuring sustained drug release. These engineered microneedles demonstrated compressive strength exceeding 0.15 N per needle, confirming their capacity for reliable skin penetration. Clinical evaluations showed that 90% of the human participants preferred monthly microneedle patches over daily oral contraceptive pills, highlighting their translational potential for improving patient compliance and self-administration [14].

4.2.5 | Musculoskeletal Disorders

Delivery to mechanically demanding tissues such as intervertebral discs presents unique challenges that require careful matching of material properties. Thread-structured microneedles have been developed for intervertebral disc repair [158] and are designed to adhere to the mechanically robust surface of the annulus fibrosus (AF) and enhance localized therapeutic delivery. By carefully matching the mechanical properties of the AF surface, these microneedles achieved superior adhesion and expanded the effective drug-release area, significantly improving therapeutic outcomes. In vivo evaluations using a rat model of intervertebral disc degeneration demonstrated that exosome-loaded thread-structured microneedles promoted AF repair by restoring mitophagy balance and maintaining extracellular matrix homeostasis. Furthermore, the microneedle system prevented nuclear pulposus extrusion, significantly reducing the risk of progressive disc degeneration. This demonstrated the pharmacokinetic advantages of direct tissue-targeted delivery for orthopedic applications.

The diverse in vivo applications discussed above highlight how structural dimensions, particularly needle length, critically determine the penetration depth, accessible biological targets, and suitable therapeutic contexts. To provide a systematic framework for matching device design to clinical requirements, Table 4 summarizes the relationship between the nano- and microneedle length scales and their biomedical applicability.

TABLE 4 | Biomedical applications of vertically aligned micro- and nanoneedle platforms.

Application	Target disease	Delivered cargo	Needle platform	Target site	Ref
Ocular disease	Retinal neovascularization, ocular disorders	Bevacizumab (Bev)	Biodegradable silicon nanostructures with high aspect ratios and porous architectures;	Cornea	[19, 20, 43, 62, 72]
Wound healing and tissue regeneration	Chronic wounds; bacterial-infected diabetic wounds	Verteporfin (VP)	Polymeric high-aspect-ratio microstructures; core–shell microneedles; biomimetic microneedle systems	Skin; wound sites	[8, 10, 11, 53]
Cancer therapy and tumor targeting	Cancer therapy; tumor targeting; mouse melanoma model	Engineered T cells; chemokine CCL22	Ice-templated polystyrene microneedles with multiple open grooves	Tumor microenvironment; tumor tissue	[12]
Metabolic disorders and contraception	Long-acting drug delivery; transdermal contraceptive delivery	Contraceptive drugs	PLA- and PLGA-based biodegradable microneedles	Skin	[13, 14]
Musculoskeletal disorders	Intervertebral disc repair; intervertebral disc degeneration	Exosomes	Thread-structured microneedles	Annulus fibrosus	[158]

5 | High-Aspect-Ratio Nanostructures for Advanced Diagnostics

The exceptional capabilities of high-aspect-ratio nanostructure technologies extend beyond therapeutic applications to the rapidly evolving field of biomedical diagnostics. These sophisticated structures can establish precise, minimally invasive interfaces with biological systems, enabling access to cellular- and tissue-level biomarkers [159]. Their unique nanoscale geometry can facilitate enhanced biomolecular interactions, efficient sample acquisition, and high-fidelity signal transduction, collectively transforming their diagnostic capabilities [160]. This section reviews the recent advances in nanostructure-based diagnostic platforms across two complementary domains: intracellular sensing systems that provide direct access to the cytoplasmic environment (Section 5.1) and tissue-integrated or wearable sensing platforms that enable continuous monitoring in dynamic physiological settings (Section 5.2).

5.1 | Intracellular Sensing: Precision Bioanalysis in Living Cells

High-aspect-ratio nanostructure platforms offer unparalleled access to the intracellular environment, enabling direct and minimally invasive monitoring of biomolecules within living cells. This unique capability allows dynamic measurement of intracellular ions, metabolites, and proteins with single-cell resolution [161]. Vertically aligned nanostructure arrays can penetrate cell membranes while preserving cellular viability, making them particularly valuable for longitudinal studies of cellular processes [5, 45, 61].

Recent studies have significantly expanded the capabilities of nanostructure-based intracellular sensing platforms. In one compelling example, Chiappini et al. developed porous silicon-nanoneedle biosensors to map the activity of intracellular cathepsin B (CTSB), a protease frequently overexpressed in malignant tumors. This system utilized TAMRA-labeled peptide substrates that are specifically cleaved by CTSB, allowing direct cytosolic sensing through fluorescence signal generation upon enzymatic cleavage (Figure 10a) [162]. When deployed in cultured cell models and human esophageal tissue samples, these nanoneedles demonstrated a remarkable capability to discriminate cancerous (CTSB-positive) cells from their noncancerous counterparts with a spatial resolution approaching single-cell precision. Thus, this platform enabled spatially resolved fluorescence detection with exceptional cellular specificity, highlighting its potential to distinguish malignant and nonmalignant cells in both research and clinical contexts.

Another advancement was demonstrated by Park et al., who introduced a transparent intracellular sensing platform combining vertically aligned silicon nanoneedles with a percolated Au–Ag nanowire network on an elastomeric substrate (Figure 10b) [163]. This device enabled simultaneous intracellular electrical recording and live-cell imaging using conventional inverted and confocal microscopy, which was previously unachievable. The platform demonstrated exceptional stability and maintained low-impedance performance for over 28 days, preserving cell viability with optical transparency. In proof-of-concept studies, this technology could successfully monitor action potentials and calcium flux in cardiomyocytes and 3D engineered cardiovascular tissues under pharmacological treatment conditions, highlighting its substantial potential for real-time physiological and pharmacological monitoring at the intracellular level.

A significant breakthrough in intracellular sensing was achieved by integrating nanoneedles with the clustered regularly interspaced short palindromic repeat (CRISPR) system and its associated proteins (Cas). Kim et al. developed nanoCRISPR, a CRISPR/Cas-assisted nanoneedle sensor that enables precise intracellular detection of adenosine triphosphate (ATP) (Figure 10c) [24]. This platform employs a two-stage detection process: initially, an aptamer-locked Cas12a activator is delivered intracellularly via nanoneedles; upon ATP binding, the activator undergoes a conformational change and becomes unlocked. Subsequently, the nanoneedles are extracted and exposed to a Cas12a detection system, which generates a fluorescence signal through collateral single-stranded DNA cleavage, enabling precise quantification of intracellular ATP. The nanoCRISPR system demonstrated high specificity with a detection limit of 246 nM while maintaining cellular viability and successfully discriminated among live, stressed, and dead cells in culture. This technology offers a way to combine the unique intracellular access provided by nanoneedles with the powerful signal-amplification capabilities of CRISPR/Cas systems to create minimally invasive yet highly sensitive approaches for intracellular molecular sensing.

In addition to these optical and molecular approaches, Abbott et al.. successfully integrated nanoneedles with complementary metal–oxide–semiconductor (CMOS) technology to develop nanoelectrode arrays for all-electrical intracellular electrophysiological imaging [164]. This platform can perform simultaneous intracellular recording across thousands of cells with high temporal and spatial resolutions. Moreover, the integration of nanoscale vertical electrodes into a CMOS architecture enhances signal sensitivity. This combination can facilitate scalable manufacturing of large-area diagnostic platforms, potentially transforming high-throughput cellular analysis for research and clinical applications.

These advancements highlight the remarkable potential of nanoneedle platforms for intracellular sensing beyond conventional static, single-point measurements. Their compatibility with multiple optical, electrochemical, and molecular signal transduction modalities, combined with minimal invasiveness, makes nanoneedles suitable for long-term, high-resolution monitoring of dynamic cellular processes across diverse biological contexts.

5.2 | Tissue-Integrated and Wearable Sensing Platforms

Beyond cellular diagnostics, high-aspect-ratio nanostructure-based systems have also been engineered into conformable, wearable, and implantable devices for real-time physiological monitoring of tissues and whole organisms. These platforms exploit the capacity of nanostructures to access the interstitial fluid or tissue microenvironments with minimal discomfort, allowing continuous biosensing in dynamic settings for extended periods. The integration of nanostructure technologies with flexible electronics, microfluidics, and wireless communication systems has opened new possibilities for decentralized healthcare monitoring and personalized diagnostics.

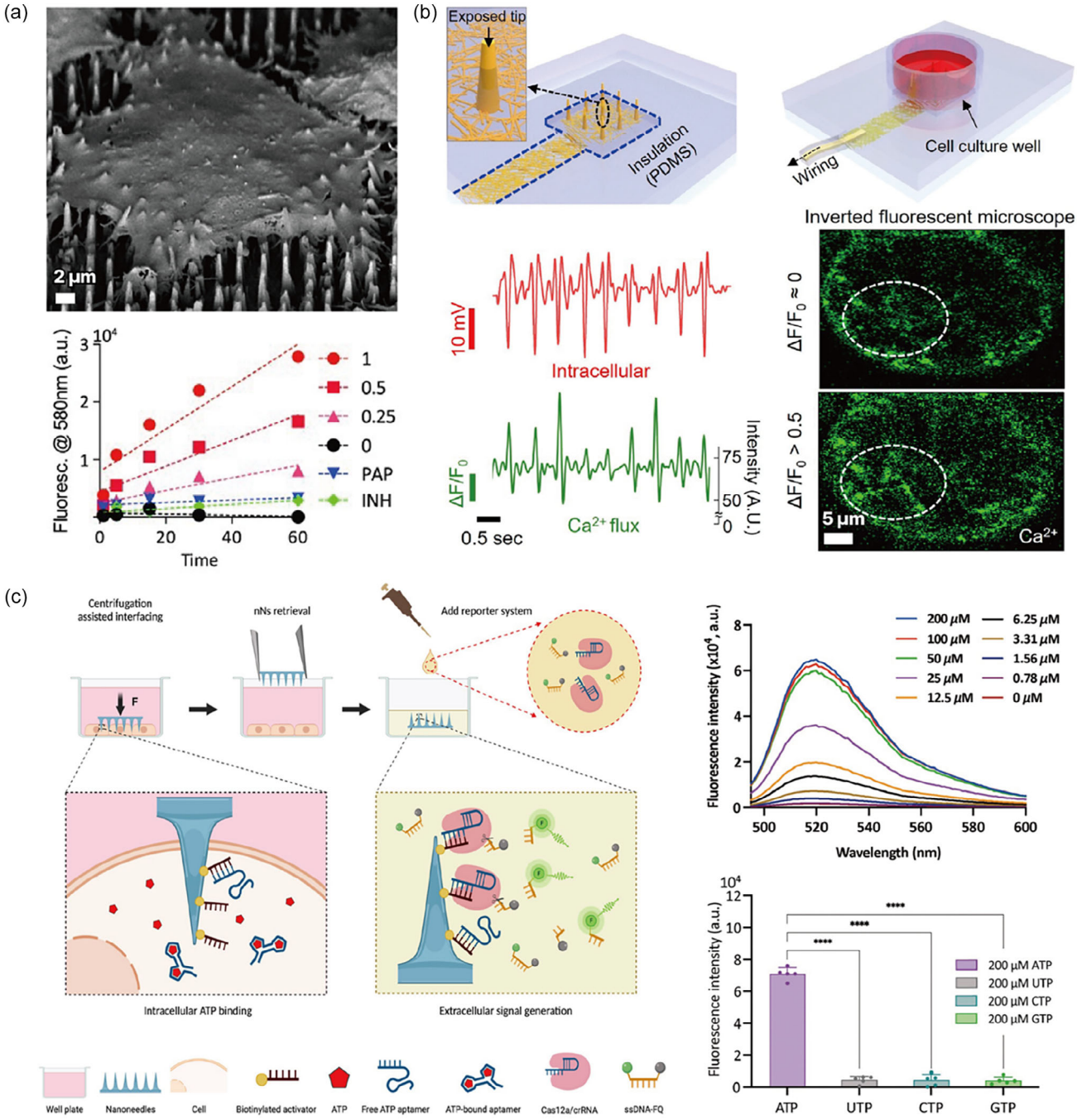

FIGURE 10 | Intracellular diagnostic applications of high-aspect-ratio nanostructures. (a) Porous silicon nanoneedles functionalized for intracellular CTSB sensing, which allow spatially resolved cancer diagnostics in human esophageal tissue. Reproduced with permission [162]. Copyright 2015, Wiley. (b) Transparent vertical silicon nanoneedles coupled with gold–silver nanowire networks for simultaneous live-cell imaging and intracellular potential recording. Reproduced with permission [163]. Copyright 2023, American Chemical Society. (c) A nanoCRISPR platform utilizing Cas12a-assisted nanoneedles for quantitative detection of ATP in living cells with high specificity. Reproduced with permission [24]. Copyright 2023, American Chemical Society.

Conformable micro- and nanostructured sensor platforms have demonstrated excellent performance in localized sensing of pathophysiological signals [165, 166]. Lee et al. presented a representative example employing siloxane-based conformable microneedles functionalized with polyaniline to enable electrochemical pH sensing for mapping peripheral artery disease (Figure 11a) [167]. The integration of dual siloxane polymers provided intimate skin adhesion and mechanical flexibility, enhancing the fidelity of signal transduction at the skin–sensor interface. This system measured the open-circuit potential between the conductive polymer-modified working electrode and a solid-state Ag/AgCl reference electrode, allowing highly sensitive detection of local acidosis. Polyaniline, which is known for its high proton sensitivity and redox activity, served as a built-in signal amplifier that translated minute pH fluctuations into measurable voltage shifts to reflect the underlying pathophysiological changes.

Another emerging development is a wearable microneedle sensor platform for continuous monitoring of levodopa (L-Dopa), the primary therapeutic agent for Parkinson disease, as demonstrated by Goud et al. (Figure 11b) [168]. This dual-mode microneedle array incorporates enzymatic and nonenzymatic detection modalities into separate microneedles within a single patch, allowing orthogonal electrochemical analysis through square-wave voltammetry and chronoamperometry. This built-in redundancy improves the specificity and robustness for detecting L-Dopa concentrations in the interstitial fluid. The device has demonstrated high sensitivity and stability over prolonged use and maintained selectivity even in the presence of biological interferents. Its functionality has been validated in skin-mimicking phantom gels and ex vivo mouse skin. This supports its translational potential for real-time, on-body pharmacokinetic monitoring to optimize Parkinson's treatment regimens.

The diagnostic capabilities of needle-based technologies were further enhanced by Yu et al., who developed an ultrathin piezoelectric microsystem that guides tissue targeting during biopsy by measuring local tissue stiffness [170]. This device integrated lead zirconate titanate (PZT) actuators and sensors onto a flexible polyimide substrate or conventional biopsy needles. The mechanical deformation induced by an applied voltage generates strain-dependent sensor voltages that quantitatively correlate with the tissue modulus upon insertion into the tissue. With a high spatial resolution, this modulus-based sensing allows precise discrimination between healthy and diseased tissues, including cancerous lesions. This approach offers real-time, mechanical property-based biopsy guidance that could substantially improve diagnostic accuracy while reducing the need for repeat procedures.

Microfluidic integration with microneedles is another major advancement in diagnostic capabilities. Xiao et al. developed a novel microfluidic-based plasmonic biosensor for ultrasensitive monitoring of uric acid in interstitial fluid (Figure 11c) [169]. This system integrated three key components: a hollow microneedle patch for fluid extraction, a flexible microfluidic chip for sample transport, and a 3D nanogold surface-enhanced Raman scattering (SERS) substrate for molecular detection. The sensor extracts subcutaneous fluid using capillary action and a manually operated suction mechanism. It routes this fluid to the sensing chamber, where uric acid is detected label-free with a remarkable detection limit of 0.51 μM. The SERS-based sensing approach exhibited exceptional selectivity and stability against a wide range of interfering biomolecules and environmental conditions. Moreover, the sensor showed reproducible uric acid detection in various skin models, including ex vivo porcine skin, and excellent agreement with commercial uric acid assay kits. These results highlight the clinical potential of such systems for personalized health monitoring and early screening for conditions such as gout and kidney dysfunction.

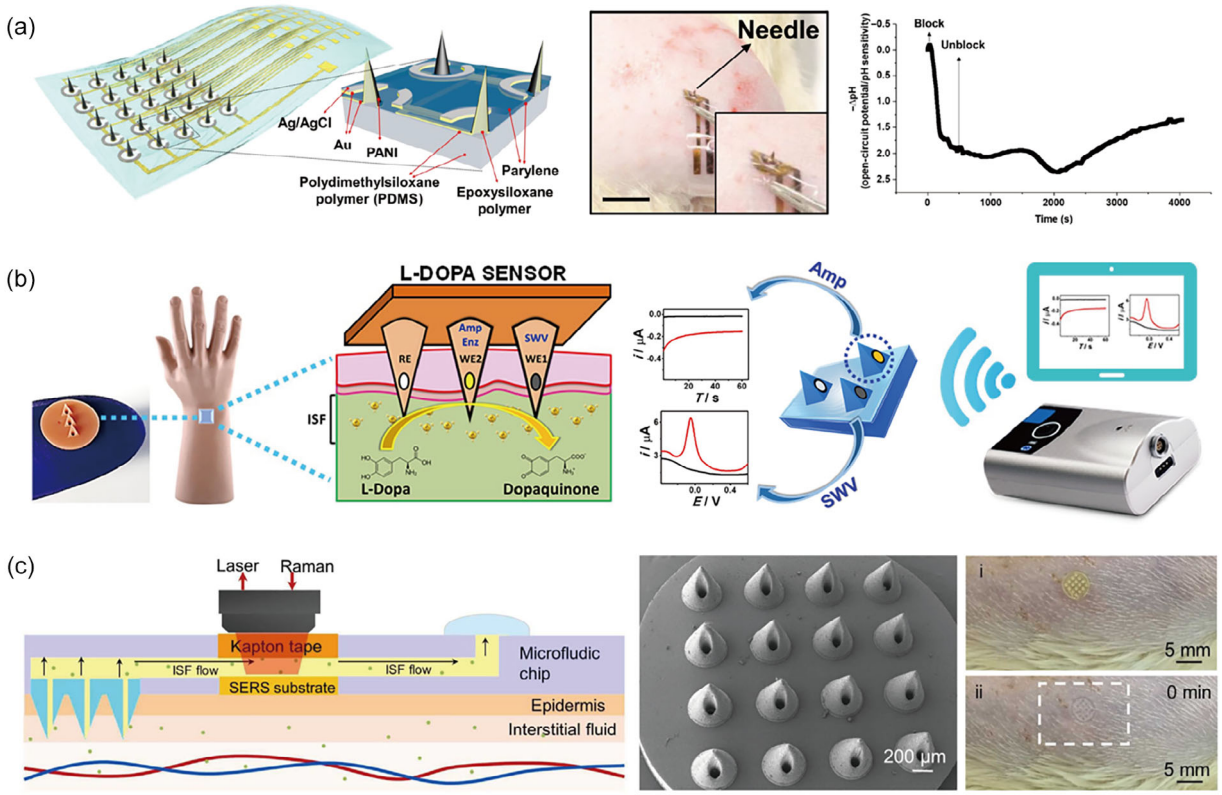

FIGURE 11 | Wearable nanostructure diagnostics for continuous health monitoring. (a) Conformable microneedle pH sensors fabricated with dual siloxane polymers for skin-adhesive, high-resolution mapping of ischemic tissues. Reproduced with permission [167]. Copyright 2021, Published by American Association for the Advancement of Science. (b) A dual-mode microneedle patch combining enzymatic and nonenzymatic electrochemical sensing for real-time L-Dopa monitoring in patients with Parkinson disease. Reproduced with permission [168]. Copyright 2019, American Chemical Society. (c) Needle-shaped ultrathin piezoelectric microsystem for real-time mechanical sensing during tissue insertion and precise discrimination between soft and stiff tissue regions. Reproduced with permission [169]. Copyright 2023, Elsevier B.V.

These examples illustrate the evolution of nanoneedle-based diagnostic platforms into multifunctional interfaces that effectively bridge the gap between soft, dynamic biological systems and high-resolution, real-time analytical technologies. Their continued integration with advanced materials, flexible electronics, microfluidics, and wireless communication networks offers the potential for personalized and decentralized healthcare monitoring across diverse clinical applications.

6 | Future Challenges and Prospects

The remarkable evolution of high-aspect-ratio nanostructure technologies over the past two decades represents a paradigm shift in biomedical device design, transforming these architectures from proof-of-concept platforms into sophisticated tools with direct applications in cell biology, therapeutic delivery, and precision diagnostics. Through advances in bottom-up, top-down, and integrative fabrication strategies, researchers have achieved unprecedented control over nanostructure geometry, mechanical properties, and surface functionalization, establishing a technological foundation for diverse applications ranging from cell mechanotransduction studies to real-time continuous biosensing.

6.1 | Emerging Opportunities and Clinical Potentials

High-aspect-ratio nanostructure technologies are rapidly advancing toward the development of next-generation biomedical devices, particularly for diagnostic [171, 172] and therapeutic-delivery applications [13, 14, 173]. Their distinctive structural characteristics, namely, micro- to nanoscale ultra-sharp tips and high aspect ratios, enable localized and minimally invasive tissue interactions that fundamentally differ from conventional millimeter-scale hypodermic needles. This difference offers a virtually pain-free alternative that supports patient self-administration and improves treatment compliance, thereby addressing one of the most important barriers to effective healthcare delivery.

The scope for continuous, noninvasive monitoring is perhaps the most noteworthy aspect of high-aspect-ratio nanostructured platforms. These devices can detect a wide range of physiological biomarkers, including pH fluctuations [72], nucleotide concentrations [24], and glucose levels [165, 174], allowing real-time health monitoring with high temporal resolution. In many implementations, mechanically robust substrates such as silicon provide the structural integrity necessary for reliable signal acquisition under physical stress, facilitating dependable sensing even under dynamic conditions or manual application. These features can expand the utility of these platforms across both clinical and self-monitoring contexts.

The development of biodegradable silicon nanostructures with porous architectures [20, 43] and microstructures fabricated from soft, biodegradable polymers [8, 9] has opened new pathways for therapeutic applications. These advanced materials enable transient tissue interfacing followed by complete biological degradation over weeks to months, eliminating the need for device retrieval and mitigating the risks associated with permanent foreign body implantation. By precisely modulating the chemical composition of the materials and incorporating customized therapeutic payloads, these platforms can be engineered for controlled, patient-specific release profiles that advance personalized medicine strategies.

6.2 | Challenges and Technological Barriers

Despite their remarkable potential, several challenges have to be addressed to fully realize the clinical transformation promised by nanostructured technologies. This section examines the critical barriers across manufacturing, regulatory approval, clinical translation, and commercial implementation that must be overcome for widespread clinical adoption.

6.2.1 | Scalable Manufacturing and Production Challenges

For economic viability and widespread clinical adoption, nanostructure technologies must be produced on an industrial scale with exceptional reliability, uniformity, and cost-effectiveness. Silicon-based platforms, while offering precise dimensional control through established semiconductor fabrication methods, show substantial cost barriers owing to their cleanroom requirements and multistep lithographic processes. To achieve commercial competitiveness with the existing delivery systems, production costs must be reduced to <$1 per device for single-use applications [175, 176].

Polymeric platforms offer more promising pathways for high-volume manufacturing through techniques such as roll-to-roll nanoimprinting and injection molding, with a demonstrated throughput exceeding 10 000 units/h [159]. However, maintaining dimensional uniformity across large substrate areas remains challenging, with typical variations of 5%–15% in needle height and diameter potentially affecting the penetration efficiency and dosing accuracy [177]. In this regard, integration of real-time quality control systems and advanced process monitoring is essential for ensuring consistent product performance at the industrial scale.

Device miniaturization and integration represent some of the most important challenges. Although recent studies have demonstrated nanostructure-integrated biosensors and drug-delivery systems in compact formats, such as smartphone-interfacing diagnostic patches and wearable monitoring devices [178], many implementations remain bulky or depend on external hardware. These limitations substantially constrain the portability and seamless integration of these platforms into daily life, hindering the transition from laboratory demonstrations to widespread clinical adoption.

6.2.2 | Regulatory Framework and Approval Pathways

The regulatory landscape for high-aspect-ratio nanostructure devices presents unique challenges owing to their combination of drug-delivery, medical-device, and potential combination-product characteristics. In the United States, microneedle-based products may fall under FDA jurisdiction as either Class II medical devices (requiring 510(k) premarket notifications) or Class III devices (requiring premarket approval), depending on their intended use and risk profile [179].

For drug-device combination products, regulatory approval requires a comprehensive demonstration of both device

performance and drug stability, bioavailability, and pharmacokinetics. Key regulatory considerations include (1) biocompatibility testing according to ISO 10993 standards, (2) demonstration of sterility and stability over product shelf life, (3) validation of consistent drug-release profiles across manufacturing lots, and (4) establishment of appropriate clinical endpoints [180]. The extended approval timeline—typically 3–7 years for novel devices—necessitates early engagement with regulatory agencies to establish appropriate testing frameworks and expediate development pathways [181].

6.2.3 | Clinical Translation Barriers

The translation from preclinical studies to human clinical trials faces several critical barriers. First, most of the published studies focused on in vitro demonstrations or acute animal studies, with limited data on long-term biocompatibility, chronic tissue responses, and clinical outcomes in humans. Second, scaling from small animal models to human applications often reveals unexpected challenges due to differences in skin thickness (human vs. mouse stratum corneum: 10–20 vs. 5–10 μm) and mechanical properties, which affect penetration efficiency and drug-delivery kinetics [182].

Long-term biocompatibility and in vivo stability present fundamental design trade-offs. Biodegradable silicon nanostructures, while engineered to degrade through controlled porosity, lack comprehensive long-term safety data on the degradation products, which are required for regulatory approval in many applications. Conversely, polymer-based platforms offer superior biocompatibility and predictable degradation pathways through FDA-approved materials (PLA and PLGA) [82, 83], but may show inadequate mechanical stability during extended implantation periods. This creates a critical consideration: biodegradable platforms may be inappropriate for long-term monitoring applications (>3 months), whereas nondegradable alternatives raise concerns regarding chronic tissue responses and require surgical removal.

The clinical trial design process presents additional challenges. Standardized application protocols must account for patient-to-patient anatomical variations. Appropriate control groups must be selected for comparison with the current standard of care, and validated biomarker endpoints must be established. Variable insertion depths, site-to-site differences in tissue properties, and difficulties in achieving reproducible dosing have limited the progress of several platforms [183]. In this regard, successful clinical translation will require the development of standardized application devices with integrated sensors for real-time monitoring and feedback control.

6.2.4 | Commercial Viability and Market Considerations

Commercial success requires not only technical performance but also favorable health economics and market positioning. Cost-effectiveness analyses must demonstrate that nanostructure-based delivery offers meaningful advantages over existing alternatives, such as improved efficacy, reduced side effects, enhanced patient compliance, and lower overall treatment costs [184].

Market adoption faces additional hurdles, including physician training requirements, establishment of reimbursement coding, and integration into clinical workflows. Self-administration applications may offer advantages in patient acceptance and healthcare cost reduction, but require intuitive device design and comprehensive patient education. Strategic partnerships among academic developers, device manufacturers, and pharmaceutical companies are essential for navigating the complex path from research innovation to commercial products, as exemplified by successful collaborations for approved microneedle vaccine-delivery systems.

6.3 | Convergent Technologies and Therapeutic Frontiers

The future of high-aspect-ratio nanostructure technologies extends far beyond current diagnostic applications, with promising opportunities in advanced therapeutic inventions and precision cellular engineering. The most powerful potential lies in the manipulation of previously challenging cell populations, particularly immune cells and neurons, which are difficult to transfect using conventional methods [7, 25, 107]. High-aspect-ratio nanostructure interfaces offer unique advantages for delivering next-generation genetic engineering tools, including advanced CRISPR systems, base editors, prime editors, and epigenome modifiers, to these sensitive cell types with minimal disruption. These approaches may also unlock new therapeutic strategies for cancer immunotherapy, neurological disorders, and regenerative medicine (Figure 12).

The evolution from fundamental mechanotransduction studies toward clinically meaningful genetic interventions represents a critical transition in the field. While early nanostructure research primarily focused on understanding the cellular responses to mechanical stimuli, future platforms should prioritize the delivery of therapeutically relevant genetic constructs to treat specific diseases. The paradigm shifts toward high-throughput, clinically applicable precision medicine could enable personalized cellular reprogramming strategies tailored to individual patient needs, moving beyond proof-of-concept demonstrations to achieve meaningful therapeutic outcomes.

Furthermore, AI-integrated nanostructure systems could enable truly personalized cellular therapies by analyzing individual patient genomics, proteomics, and cellular phenotypes to design customized genetic interventions. These sophisticated systems could potentially revolutionize the treatment of complex diseases such as cancer, where heterogeneous cellular populations require precisely tailored therapeutic approaches. The integration of nanostructure technologies with Internet of Things (IoT) architectures and cloud-based healthcare systems promises distributed therapeutic monitoring networks that can fundamentally transform treatment delivery and optimization, provide real-time feedback on therapeutic efficacy, and enable dynamic adjustment of treatment protocols.

7 | Conclusion and Future Roadmap

7.1 | Current State and Achievements

High-aspect-ratio nanostructure technologies have evolved from fundamental research tools to sophisticated platforms with direct clinical applications. This field has achieved remarkable milestones: fabrication methods enabling sub-10-nm resolution

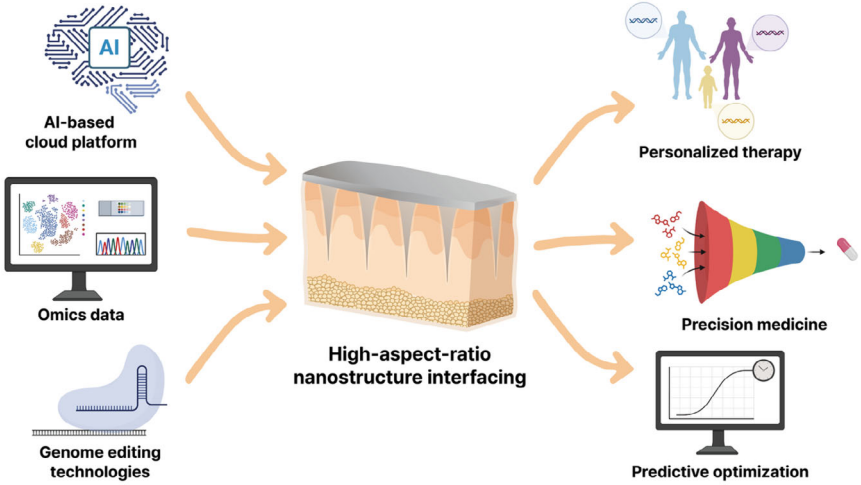

FIGURE 12 | The integration of high-aspect-ratio nanostructure technologies with AI and genome editing can offer a transformative platform for next-generation precision medicine through individualized, adaptive therapeutic interventions.

through e-beam lithography [36], intracellular delivery efficiencies exceeding 90% [61], and diagnostic platforms capable of single-cell resolution [24, 162–164]. Applications spanning mechanotransduction studies, genetic engineering delivery, and continuous biosensing have demonstrated the technical feasibility of these platforms and established proof-of-concept for clinical translation. Despite these achievements, substantial gaps remain between laboratory demonstrations and widespread clinical adoption, particularly in terms of scalable manufacturing, regulatory approval, and long-term clinical validation.

7.2 | Research Priorities

Accelerating clinical translation requires addressing the interconnected challenges across technology development, regulatory approval, and commercial implementation. We propose the following research priorities organized according to realistic timelines.

7.2.1 | Immediate Priorities (1–2 Years)

- Development of standardized characterization protocols for comparing nanostructure performance across platforms, including quantitative benchmarks for penetration efficiency, delivery kinetics, and cellular responses
- Comprehensive biocompatibility studies in accordance with ISO 10993 standards, with standardized endpoints for acute toxicity, chronic tissue response, and degradation product clearance
- Cost-reduction strategies targeting costs <$5 per device through process optimization and alternative fabrication approaches
- Establishment of multiinstitutional collaborations for pooling clinical data and testing protocols

7.2.2 | Short-Term Goals (2–3 Years)

- Completion of long-term stability studies (>6 months) for biodegradable platforms under physiologically relevant conditions, establishing degradation kinetics and mechanical integrity timelines
- Integration of sensing capabilities for real-time monitoring of drug release, tissue response, and therapeutic efficacy, thereby enabling closed-loop feedback systems.
- Initiation of phase I clinical trials for lead applications, including transdermal delivery, ocular therapeutics, and vaccine administration
- Development of applicator devices with integrated quality control (depth sensors and force feedback) to ensure reproducible clinical administration.

7.2.3 | Medium-Term Targets (3–5 Years)

- FDA approval of first-generation nanostructure-based drug-delivery products
- Demonstration of clinical superiority through phase II/III trials showing improved patient outcomes in comparison with current standards of care (reduced dosing frequency, enhanced efficacy, and fewer adverse events)
- Establishment of large-scale manufacturing with >90% yield efficiency and minimized dimensional variation to meet the regulatory requirements for commercial production.
- Integration with digital healthcare platforms for remote patient management and telemedicine applications

7.2.4 | Long-Term Vision (5–10 Years)

- Development of AI-integrated personalized therapeutic platforms that customize the nanostructure design, drug loading, and release kinetics on the basis of individual patient genomics, cellular phenotypes, and real-time physiological feedback
- Widespread clinical adoption across multiple therapeutic domains, including cancer immunotherapy (CAR-T delivery), neurological disorders (neural interface devices), and chronic disease management (continuous monitoring and on-demand delivery)

- Expansion to advanced applications combining gene editing (CRISPR/base editors) and nanostructure delivery for previously intractable genetic diseases
- Market maturation with multiple FDA-approved products achieving significant clinical penetration in target indications

7.3 | Future Opportunities

Realizing the roadmap outlined above requires convergence with several emerging technologies that will amplify nanostructure capabilities.

7.3.1 | AI and Machine Learning Integration

Coupling nanostructure platforms with AI algorithms promises advances in treatment optimization. Machine learning models trained on cellular-response data can predict the optimal structural parameters (geometry, surface chemistry, and drug loading) for specific cell types and therapeutic cargoes, reducing the empirical optimization time from months to days. Real-time adaptive systems can continuously adjust drug-release rates on the basis of biosensor feedback, thereby maintaining therapeutic levels while minimizing side effects, which will be particularly valuable for cancer therapy and chronic disease management.

7.3.2 | Advanced Genetic Engineering Tools

The most significant opportunities lie in harnessing next-generation cellular engineering using nanostructure platforms, particularly for previously inaccessible cell populations such as immune cells and neurons. By enabling precise delivery of advanced genetic tools, including CRISPR systems and epigenome editors, these platforms could unlock novel therapeutic paradigms for treating cancer, neurological disorders, and immune-related diseases with unprecedented specificity and efficacy. Particularly promising targets are as follows:

- CAR-T cell engineering: Direct delivery of genetic circuits for enhanced tumor targeting and reduced exhaustion
- Neural repair: Delivery of regenerative factors and guidance molecules for treating neurodegenerative diseases
- In vivo gene therapy: Tissue-specific delivery avoiding viral vector limitations

7.3.3 | Internet of Medical Things

The integration of nanostructure-based sensors with wireless communication and cloud analytics can enable the development of distributed health-monitoring networks. Continuous transmission of biosensor data to cloud platforms can provide predictive diagnostics, identify pathological changes before symptom onset, and enable proactive intervention rather than reactive treatment. This paradigm shift from episodic to continuous care represents a fundamental transformation in healthcare delivery.

7.4 | Concluding Remarks

The roadmap and timeline presented in Figure 13 provide a realistic pathway for translating high-aspect-ratio nanostructure technologies from current achievements to transformative clinical impact. The success of these attempts will depend on sustained interdisciplinary collaboration among materials scientists, biomedical engineers, clinicians, regulatory specialists, and industry partners, each contributing essential expertise to navigate the complex journey from bench to bedside.

The field of high-aspect-ratio nanostructure technology research is at a critical juncture. Technical capabilities have matured sufficiently to address real clinical needs, yet systematic barriers to manufacturing, regulation, and clinical validation remain. By pursuing the concrete milestones outlined here, the community can systematically overcome these barriers while focusing on patient benefit as the ultimate measure of success.

As we advance along this path, high-aspect-ratio nanostructures have the potential to establish new paradigms in precision medicine, enabling earlier disease detection, more effective targeted therapies, and truly personalized treatment strategies that fundamentally improve the diagnosis, monitoring, and treatment of

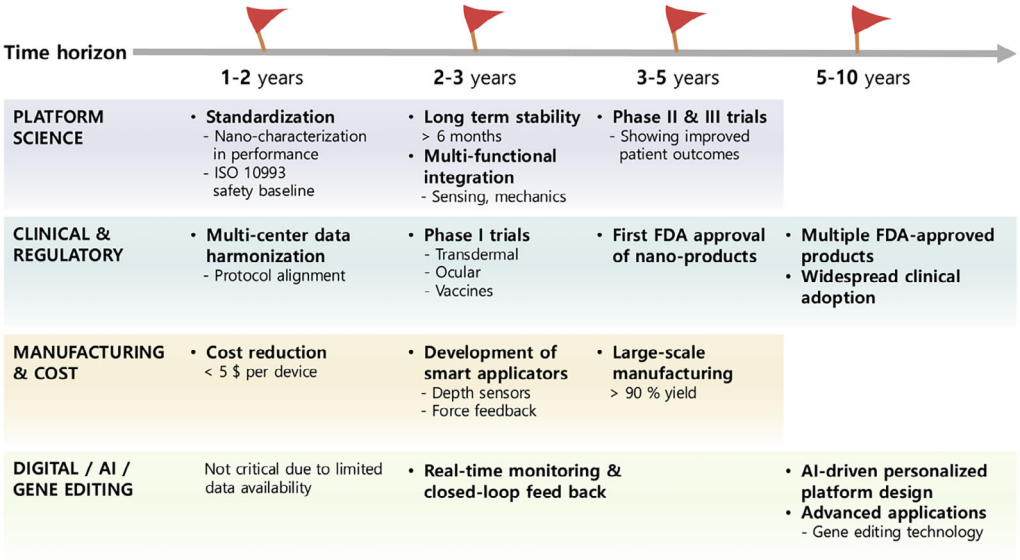

FIGURE 13 | Roadmap for clinical translation of high-aspect-ratio nanostructures.

diseases. The next decade will be critical for determining whether these promising technologies can fulfill their potential to transform healthcare delivery and patient outcomes.

Author Contributions

Yerim Jang: conceptualization (equal), data curation (equal), investigation (equal), visualization (equal), writing – original draft (equal), writing – review and editing (equal). **Sowon Lee:** investigation (supporting), visualization (supporting), writing – original draft (supporting), writing – review and editing (supporting). **Younghak Cho:** conceptualization (equal), data curation (equal), investigation (equal), validation (equal), visualization (equal), writing – original draft (equal), writing – review and editing (equal). **Hyejeong Seong:** conceptualization (lead), investigation (lead), project administration (lead), supervision (lead), visualization (supporting), writing – original draft (lead), writing – review and editing (lead)

Acknowledgments

This research was supported by the National R&D Program through the National Research Foundation of Korea (NRF), funded by the Ministry of Science and ICT (Grant No. RS-2025-00517552), and by KIST research programs (2E33682 and 2E33712).

Funding

This study was supported by the National Research Foundation of Korea (RS-2025−00517552) and the Korea Institute of Science and Technology (2E33682 and 2E33712).

Conflicts of Interest

The authors declare no conflicts of interest.

Data Availability Statement

The data supporting the findings of this study are available from the corresponding author upon reasonable request.

References

1. M. Balash, H. Boucetta, and W. He, "Factors Affecting Drug Delivery System Translation: A Focus on Advanced Technologies, Biological Barriers, and Regulatory Challenges," *Journal of Controlled Release* 387 (2025): 114167, https://doi.org/10.1016/j.jconrel.2025.114167.

2. G. L. Zheng, B. Zhang, H. Y. Yu, et al., "Therapeutic Applications and Potential Biological Barriers of Nano-Delivery Systems in Common Gastrointestinal Disorders: A Comprehensive Review," *Advanced Composites and Hybrid Materials* 8, no. 2 (2025): 227, https://doi.org/10.1007/s42114-025-01292-3.

3. Z. Cheng, H. Huang, M. Yin, and H. Liu, "Applications of Liposomes and Lipid Nanoparticles in Cancer Therapy: Current Advances and Prospects," *Experimental Hematology & Oncology* 14, no. 1 (2025): 11, https://doi.org/10.1186/s40164-025-00602-1.

4. J. Carthew, H. H. Abdelmaksoud, K. J. Cowley, et al., "Next Generation Cell Culture Tools Featuring Micro- and Nanotopographies for Biological Screening," *Advanced Functional Materials* 32, no. 3 (2021): 2100881, https://doi.org/10.1002/adfm.202100881.

5. G. He, N. Hu, A. M. Xu, et al., "Nanoneedle Platforms: The Many Ways to Pierce the Cell Membrane," *Advanced Functional Materials* 30, no. 21 (2020): 1909890, https://doi.org/10.1002/adfm.201909890.

6. Z. Liu, J. Nie, B. Miao, et al., "Self-Powered Intracellular Drug Delivery by a Biomechanical Energy-Driven Triboelectric Nanogenerator," *Advanced Materials* 31, no. 12 (2019): e1807795, https://doi.org/10.1002/adma.201807795.

7. X. Liu, J. Jiang, J. Liu, et al., "Nanoneedle Array-Electroporation Facilitates Intranuclear Ribonucleoprotein Delivery and High Throughput Gene Editing," *Advanced Healthcare Materials* 13, no. 29 (2024): e2400645, https://doi.org/10.1002/adhm.202400645.

8. Z. Zhu, J. Wang, X. Pei, et al., "Blue-Ringed Octopus-Inspired Microneedle Patch for Robust Tissue Surface Adhesion and Active Injection Drug Delivery," *Science Advances* 9, no. 25 (2023): eadh2213, https://doi.org/10.1126/sciadv.adh2213.

9. Y. Zhang, S. Wang, Y. Yang, et al., "Scarless Wound Healing Programmed by Core-Shell Microneedles," *Nature Communications* 14, no. 1 (2023): 3431, https://doi.org/10.1038/s41467-023-39129-6.

10. T. Waghule, G. Singhvi, S. K. Dubey, et al., "Microneedles: A Smart Approach and Increasing Potential for Transdermal Drug Delivery System," *Biomedicine & Pharmacotherapy* 109 (2019): 1249–1258, https://doi.org/10.1016/j.biopha.2018.10.078.

11. L. Long, D. Ji, C. Hu, et al., "Microneedles for In Situ Tissue Regeneration," *Materials Today Bio* 19 (2023): 100579, https://doi.org/10.1016/j.mtbio.2023.100579.

12. R. Zhou, H. Yu, T. Sheng, et al., "Grooved Microneedle Patch Augments Adoptive T Cell Therapy Against Solid Tumors via Diverting Regulatory T Cells," *Advanced Matererials* 36, no. 30 (2024): e2401667, https://doi.org/10.1002/adma.202401667.

13. W. Li, R. N. Terry, J. Tang, et al., "Rapidly Separable Microneedle Patch for the Sustained Release of a Contraceptive," *Nature Biomedical Engineering* 3, no. 3 (2019): 220–229, https://doi.org/10.1038/s41551-018-0337-4.

14. W. Li, J. Tang, R. N. Terry, et al., "Long-Acting Reversible Contraception by Effervescent Microneedle Patch," *Science Advances* 5, no. 11 (2019): eaaw8145, https://doi.org/10.1126/sciadv.aaw8145.

15. E. Lestrell, Y. Chen, S. Aslanoglou, et al., "Silicon Nanoneedle-Induced Nuclear Deformation: Implications for Human Somatic and Stem Cell Nuclear Mechanics," *ACS Applied Materials & Interfaces* 14, no. 40 (2022): 45124–45136, https://doi.org/10.1021/acsami.2c10583.

16. H. Seong, S. G. Higgins, J. Penders, et al., "Size-Tunable Nanoneedle Arrays for Influencing Stem Cell Morphology, Gene Expression, and Nuclear Membrane Curvature," *ACS Nano* 14, no. 5 (2020): 5371–5381, https://doi.org/10.1021/acsnano.9b08689.

17. Y. Zeng, Y. Zhuang, B. Vinod, et al., "Guiding Irregular Nuclear Morphology on Nanopillar Arrays for Malignancy Differentiation in Tumor Cells," *Nano Letters* 22, no. 18 (2022): 7724–7733, https://doi.org/10.1021/acs.nanolett.2c01849.

18. S. Park, H. H. Park, K. Sun, et al., "Hydrogel Nanospike Patch as a Flexible Anti-Pathogenic Scaffold for Regulating Stem Cell Behavior," *ACS Nano* 13, no. 10 (2019): 11181–11193, https://doi.org/10.1021/acsnano.9b04109.

19. C. Chiappini, E. De Rosa, J. O. Martinez, et al., "Biodegradable Silicon Nanoneedles Delivering Nucleic Acids Intracellularly Induce Localized In Vivo Neovascularization," *Nature Materials* 14, no. 5 (2015): 532–539, https://doi.org/10.1038/nmat4249.

20. W. Park, V. P. Nguyen, Y. Jeon, et al., "Biodegradable Silicon Nanoneedles for Ocular Drug Delivery," *Science Advances* 8, no. 13 (2022): eabn1772, https://doi.org/10.1126/sciadv.abn1772.

21. D. Hachim, J. Zhao, J. Bhankharia, et al., "Polysaccharide-Polyplex Nanofilm Coatings Enhance Nanoneedle-Based Gene Delivery and Transfection Efficiency," *Small* 18, no. 36 (2022): e2202303, https://doi.org/10.1002/smll.202202303.

22. Y. Liu, J. Wang, X. Huang, et al., "Glutathione-Sensitive Silicon Nanowire Arrays for Gene Transfection," *ACS Applied Materials & Interfaces* 11, no. 50 (2019): 46515–46524, https://doi.org/10.1021/acsami.9b17006.

23. X. Li, Y. Ma, Y. Xue, et al., "High-Throughput and Efficient Intracellular Delivery Method via a Vibration-Assisted Nanoneedle/Microfluidic Composite System," *ACS Nano* 17, no. 3 (2023): 2101–2113, https://doi.org/10.1021/acsnano.2c07852.

24. H. Kim, C. Gu, S. A. Mustfa, et al., "CRISPR/Cas-Assisted Nanoneedle Sensor for Adenosine Triphosphate Detection in Living Cells," *ACS Applied Materials & Interfaces* 15, no. 43 (2023): 49964–49973, https://doi.org/10.1021/acsami.3c07918.

25. N. Sun, C. Wang, W. Edwards, et al., "Nanoneedle-Based Electroporation for Efficient Manufacturing of Human Primary Chimeric Antigen Receptor Regulatory T-Cells," *Advanced Science* 12, no. 21 (2025): e2416066, https://doi.org/10.1002/advs.202416066.

26. M. Rahamathulla, S. Murugesan, D. V. Gowda, et al., "The Use of Nanoneedles in Drug Delivery: An Overview of Recent Trends and Applications," *AAPS PharmSciTech* 24, no. 8 (2023): 216, https://doi.org/10.1208/s12249-023-02661-1.

27. B. Liu, X. Yi, Y. Zheng, et al., "A Review of Nano/Micro/Milli Needles Fabrications for Biomedical Engineering," *Chinese Journal of Mechanical Engineering* 35, no. 1 (2022): 106, https://doi.org/10.1186/s10033-022-00773-6.

28. M. J. Kim, B. Lee, K. Yang, et al., "BMP-2 Peptide-Functionalized Nanopatterned Substrates for Enhanced Osteogenic Differentiation of Human Mesenchymal Stem Cells," *Biomaterials* 34, no. 30 (2013): 7236–7246, https://doi.org/10.1016/j.biomaterials.2013.06.019.

29. K. Yang, S. J. Yu, J. S. Lee, et al., "Electroconductive Nanoscale Topography for Enhanced Neuronal Differentiation and Electrophysiological Maturation of Human Neural Stem Cells," *Nanoscale* 9, no. 47 (2017): 18737–18752, https://doi.org/10.1039/c7nr05446g.

30. G. Hazell, P. W. May, P. Taylor, et al., "Studies of Black Silicon and Black Diamond as Materials for Antibacterial Surfaces," *Biomaterials Science* 6, no. 6 (2018): 1424–1432, https://doi.org/10.1039/c8bm00107c.

31. S. N. Mohammad, "The VLS Mechanism," in *Synthesis of Nanomaterials*, ed. S. N. Mohammad (Springer International Publishing, 2020), 69–99, https://doi.org/10.1007/978-3-030-57585-4_5.

32. J. Kwon, J. S. Lee, J. Lee, et al., "Vertical Nanowire Electrode Array for Enhanced Neurogenesis of Human Neural Stem Cells via Intracellular Electrical Stimulation," *Nano Letters* 21, no. 14 (2021): 6343–6351, https://doi.org/10.1021/acs.nanolett.0c04635.

33. X. P. Shen, M. Han, J. M. Hong, Z. L. Xue, and Z. Xu, "Template-Based CVD Synthesis of ZnS Nanotube Arrays," *Chemical Vapor Deposition* 11, no. 5 (2005): 250–253, https://doi.org/10.1002/cvde.200406350.

34. R. Wen, A. H. Zhang, D. Liu, et al., "Intracellular Delivery and Sensing System Based on Electroplated Conductive Nanostraw Arrays," *ACS Applied Materials & Interfaces* 11, no. 47 (2019): 43936–43948, https://doi.org/10.1021/acsami.9b15619.

35. A. E. Mironov, J. Kim, Y. Huang, et al., "Photolithography in the Vacuum Ultraviolet (172 nm) with Sub-400 nm Resolution: Photoablative Patterning of Nanostructures and Optical Components in Bulk Polymers and Thin Films on Semiconductors," *Nanoscale* 12, no. 32 (2020): 16796–16804, https://doi.org/10.1039/d0nr04142d.

36. N. Qin, Z. G. Qian, C. Zhou, X. X. Xia, and T. H. Tao, "3D Electron-Beam Writing at Sub-15 nm Resolution Using Spider Silk as a Resist," *Nature Communications* 12, no. 1 (2021): 5133, https://doi.org/10.1038/s41467-021-25470-1.

37. K. S. Beckwith, S. Ullmann, J. Vinje, and P. Sikorski, "Influence of Nanopillar Arrays on Fibroblast Motility, Adhesion, and Migration Mechanisms," *Small* 15, no. 43 (2019): e1902514, https://doi.org/10.1002/smll.201902514.

38. Y. P. Chen, M. Mach, A. R. Shokouhi, et al., "Efficient Non-Viral CAR-T Cell Generation via Silicon-Nanotube-Mediated Transfection," *Materials Today* 63 (2023): 8–17, https://doi.org/10.1016/j.mattod.2023.02.009.

39. Y. Chen, S. Aslanoglou, T. Murayama, et al., "Silicon-Nanotube-Mediated Intracellular Delivery Enables Ex Vivo Gene Editing," *Advanced Materials* 32, no. 24 (2020): e2000036, https://doi.org/10.1002/adma.202000036.

40. A. X. Pan, M. Samaan, Z. Yan, W. H. Hu, and B. Cui, "Fabrication of Ultrahigh Aspect Ratio Si Nanopillar and Nanocone Arrays," *Journal of Vacuum Science & Technology B* 41, no. 2 (2023): 023001, https://doi.org/10.1116/6.0002276.

41. C. J. Li, Y. X. Yang, R. Qu, et al., "Recent Advances in Plasma Etching for Micro and Nano Fabrication of Silicon-Based Materials: A Review," *Journal of Materials Chemistry C* 12, no. 45 (2024): 18211–18237, https://doi.org/10.1039/d4tc00612g.

42. E. A. Hussein, B. Rice, and R. J. White, "Tuning the Probe-Bilayer Architecture of Silver Nanoneedle-Based Ion Channel Probes," *Langmuir* 40, no. 13 (2024): 7234–7241, https://doi.org/10.1021/acs.langmuir.4c00454.

43. C. Wang, C. Gu, C. Popp, et al., "Integrating Porous Silicon Nanoneedles Within Medical Devices for Nucleic Acid Nanoinjection," *ACS Nano* 18, no. 23 (2024): 14938–14953, https://doi.org/10.1021/acsnano.4c00206.

44. Z. Jahed, Y. Yang, C. T. Tsai, et al., "Nanocrown Electrodes for Parallel and Robust Intracellular Recording of Cardiomyocytes," *Nature Communications* 13, no. 1 (2022): 2253, https://doi.org/10.1038/s41467-022-29726-2.

45. Y. Jang, Y. Cho, H. J. Cho, et al., "Mechanically Flexible Polymeric Nanoneedle Arrays for Promoting Differentiation and Functional Activity of Neural Progenitor Cells," *Biochip Journal* 19, no. 2 (2025): 313–323, https://doi.org/10.1007/s13206-025-00194-2.

46. S. Terashima, C. Tatsukawa, M. Suzuki, T. Takahashi, and S. Aoyagi, "Fabrication of Microneedle Using Poly Lactic Acid Sheets by Thermal Nanoimprint," *Precision Engineering* 59 (2019): 110–119, https://doi.org/10.1016/j.precisioneng.2019.05.015.

47. H. Z. Yoh, Y. Chen, S. Aslanoglou, et al., "Polymeric Nanoneedle Arrays Mediate Stiffness-Independent Intracellular Delivery," *Advanced Functional Materials* 32, no. 3 (2021): 2104828, https://doi.org/10.1002/adfm.202104828.

48. A. Sadeqi, G. Kiaee, W. Zeng, H. Rezaei Nejad, and S. Sonkusale, "Hard Polymeric Porous Microneedles on Stretchable Substrate for Transdermal Drug Delivery," *Scientific Reports* 12, no. 1 (2022): 1853, https://doi.org/10.1038/s41598-022-05912-6.

49. A. Jacobo-Martin, N. Jost, J. J. Hernandez, et al., "Roll-to-Roll Nanoimprint Lithography of High Efficiency Fresnel Lenses for Micro-Concentrator Photovoltaics," *Optics Express* 29, no. 21 (2021): 34135–34149, https://doi.org/10.1364/OE.437803.

50. M. Modaresialam, Z. Chehadi, T. Bottein, M. Abbarchi, and D. Grosso, "Nanoimprint Lithography Processing of Inorganic-Based Materials," *Chemistry of Materials* 33, no. 14 (2021): 5464–5482, https://doi.org/10.1021/acs.chemmater.1c00693.

51. S. Luo, B. H. Hoff, S. A. Maier, and J. C. de Mello, "Scalable Fabrication of Metallic Nanogaps at the Sub-10 nm Level," *Advanced Science* 8, no. 24 (2021): e2102756, https://doi.org/10.1002/advs.202102756.

52. M. J. Haslinger, O. S. Maier, M. Pribyl, et al., "Increasing the Stability of Isolated and Dense High-Aspect-Ratio Nanopillars Fabricated Using UV-Nanoimprint Lithography," *Nanomaterials* 13, no. 9 (2023): 1556, https://doi.org/10.3390/nano13091556.

53. Y. H. Liu, C. F. He, T. H. Qiao, et al., "Coral-Inspired Hollow Microneedle Patch with Smart Sensor Therapy for Wound Infection," *Advanced Functional Materials* 34, no. 24 (2024): 2314071, https://doi.org/10.1002/adfm.202314071.

54. Z. Wang, J. Luan, A. Seth, et al., "Microneedle Patch for the Ultrasensitive Quantification of Protein Biomarkers in Interstitial

Fluid," *Nature Biomedical Engineering* 5, no. 1 (2021): 64–76, https://doi.org/10.1038/s41551-020-00672-y.

55. M. Friedl, K. Cerveny, P. Weigele, et al., "Template-Assisted Scalable Nanowire Networks," *Nano Letters* 18, no. 4 (2018): 2666–2671, https://doi.org/10.1021/acs.nanolett.8b00554.

56. V. G. Dubrovskii, W. Kim, V. Piazza, L. Guniat, and I. M. A. Fontcuberta, "Simultaneous Selective Area Growth of Wurtzite and Zincblende Self-Catalyzed GaAs Nanowires on Silicon," *Nano Letters* 21, no. 7 (2021): 3139–3145, https://doi.org/10.1021/acs.nanolett.1c00349.

57. B. P. Isaacoff and K. A. Brown, "Progress in Top-Down Control of Bottom-Up Assembly," *Nano Letters* 17, no. 11 (2017): 6508–6510, https://doi.org/10.1021/acs.nanolett.7b04479.

58. S. E. Jung, J. W. Shin, Y. J. Han, and B. J. Choi, "Self-Assembled Monolayers in Area-Selective Atomic Layer Deposition and Their Challenges," *Journal of Powder Materials* 32, no. 3 (2025): 179–190, https://doi.org/10.4150/jpm.2025.00094.

59. E. Gonzalez Solveyra, D. H. Thompson, and I. Szleifer, "Proteins Adsorbing onto Surface-Modified Nanoparticles: Effect of Surface Curvature, pH, and the Interplay of Polymers and Proteins Acid-Base Equilibrium," *Polymers* 14, no. 4 (2022): 739, https://doi.org/10.3390/polym14040739.

60. L. Wang, C. Li, C. Cao, et al., "Multifunctional Polymeric Nanoneedles with "Full-Spectrum Intrinsic Internal Standard" for Precise SERS Biosensing," *Advanced Functional Materials* 35, no. 10 (2024): 2416789, https://doi.org/10.1002/adfm.202416789.

61. Y. Cho, S. Kim, H. J. Cho, et al., "Cellular Nanointerface of Vertical Nanostructures: Impact of Size-Modulated Nanopillar Arrays on Neuronal Morphology, Maturation, and Synapse Formation," *Small Structures* 6, no. 1 (2025): 2400314, https://doi.org/10.1002/sstr.202400314.

62. H. Kim, H. Jang, B. Kim, et al., "Flexible Elastomer Patch with Vertical Silicon Nanoneedles for Intracellular and Intratissue Nanoinjection of Biomolecules," *Science Advances* 4, no. 11 (2018): eaau6972, https://doi.org/10.1126/sciadv.aau6972.

63. C. Chiappini, Y. Chen, S. Aslanoglou, et al., "Tutorial: Using Nanoneedles for Intracellular Delivery," *Nature Protocols* 16, no. 10 (2021): 4539–4563, https://doi.org/10.1038/s41596-021-00600-7.

64. T. Peng, Y. Chen, X. Luan, et al., "Microneedle Technology for Enhanced Topical Treatment of Skin Infections," *Bioactive Materials* 45 (2025): 274–300, https://doi.org/10.1016/j.bioactmat.2024.11.027.

65. Y. Yin, L. Tang, Y. Cao, et al., "Microneedle Patch-Involved Local Therapy Synergized with Immune Checkpoint Inhibitor for Pre- and Post-Operative Cancer Treatment," *Journal of Controlled Release* 379 (2025): 678–695, https://doi.org/10.1016/j.jconrel.2025.01.051.

66. S. Hu, Z. Li, D. Zhu, et al., "Microneedle Delivery of Small Extracellular Vesicles From Young Blood to Treat Endothelial Senescence," *Advanced Materials* 38 (2025): e2418352, https://doi.org/10.1002/adma.202418352.

67. L. Tang, H. N. Liu, Y. Yin, et al., "Micro/Nano System-Mediated Local Treatment in Conjunction with Immune Checkpoint Inhibitor against Advanced-Stage malignant Melanoma," *Chemical Engineering Journal* 497 (2024): 154499, https://doi.org/10.1016/j.cej.2024.154499.

68. M. A. Hopcroft, W. D. Nix, and T. W. Kenny, "What Is the Young's Modulus of Silicon?," *Journal of Microelectromechanical Systems* 19, no. 2 (2010): 229–238, https://doi.org/10.1109/jmems.2009.2039697.

69. Y. Calahorra, O. Shtempluck, V. Kotchetkov, and Y. E. Yaish, "Young's Modulus, Residual Stress, and Crystal Orientation of Doubly Clamped Silicon Nanowire Beams," *Nano Letters* 15, no. 5 (2015): 2945–2950, https://doi.org/10.1021/nl5047939.

70. J. J. VanDersarl, A. M. Xu, and N. A. Melosh, "Nanostraws for Direct Fluidic Intracellular Access," *Nano Letters* 12, no. 8 (2012): 3881–3886, https://doi.org/10.1021/nl204051v.

71. S. Gopal, C. Chiappini, J. Penders, et al., "Porous Silicon Nanoneedles Modulate Endocytosis to Deliver Biological Payloads," *Advanced Materials* 31, no. 12 (2019): e1806788, https://doi.org/10.1002/adma.201806788.

72. C. Chiappini, J. O. Martinez, E. De Rosa, et al., "Biodegradable Nanoneedles for Localized Delivery of Nanoparticles In Vivo: Exploring the Biointerface," *ACS Nano* 9, no. 5 (2015): 5500–5509, https://doi.org/10.1021/acsnano.5b01490.

73. N. Sargioti, T. J. Levingstone, E. D. O'Cearbhaill, H. O. McCarthy, and N. J. Dunne, "Metallic Microneedles for Transdermal Drug Delivery: Applications, Fabrication Techniques and the Effect of Geometrical Characteristics," *Bioengineering* 10, no. 1 (2022): 24, https://doi.org/10.3390/bioengineering10010024.

74. X. Dou, L. L. Liu, and X. J. Zhu, "Nickel-Elicited Systemic Contact Dermatitis," *Contact Dermatitis* 48, no. 3 (2003): 126–129, https://doi.org/10.1034/j.1600-0536.2003.00017.x.

75. A. Spanu, N. Colistra, P. Farisello, et al., "A Three-Dimensional Micro-Electrode Array for in-Vitro Neuronal Interfacing," *Journal of Neural Engineering* 17, no. 3 (2020): 036033, https://doi.org/10.1088/1741-2552/ab9844.

76. P. Wijdenes, K. Haider, C. Gavrilovici, et al., "Three Dimensional Microelectrodes Enable High Signal and Spatial Resolution for Neural Seizure Recordings in Brain Slices and Freely Behaving Animals," *Scientific Reports* 11, no. 1 (2021): 21952, https://doi.org/10.1038/s41598-021-01528-4.

77. M. N. Kavaldzhiev, J. E. Perez, R. Sougrat, et al., "Inductively Actuated Micro Needles for on-Demand Intracellular Delivery," *Scientific Reports* 8, no. 1 (2018): 9918, https://doi.org/10.1038/s41598-018-28194-3.

78. S. Park, S. O. Choi, S. J. Paik, et al., "Intracellular Delivery of Molecules Using Microfabricated Nanoneedle Arrays," *Biomedical Microdevices* 18, no. 1 (2016): 10, https://doi.org/10.1007/s10544-016-0038-2.

79. Y. Chen, S. Aslanoglou, G. Gervinskas, et al., "Cellular Deformations Induced by Conical Silicon Nanowire Arrays Facilitate Gene Delivery," *Small* 15, no. 47 (2019): e1904819, https://doi.org/10.1002/smll.201904819.

80. A. K. Shalek, J. T. Robinson, E. S. Karp, et al., "Vertical Silicon Nanowires as a Universal Platform for Delivering Biomolecules into Living Cells," *Proceedings of the National Academy of Sciences of the United States of America* 107, no. 5 (2010): 1870–1875, https://doi.org/10.1073/pnas.0909350107.

81. W. Li, Y. Qiu, L. Zhang, et al., "Aluminum Nanopyramid Array with Tunable Ultraviolet-Visible-Infrared Wavelength Plasmon Resonances for Rapid Detection of Carbohydrate Antigen 199," *Biosensors and Bioelectronics* 79 (2016): 500–507, https://doi.org/10.1016/j.bios.2015.12.038.

82. B. Xia, Y. Liu, Y. Xing, Z. Shi, and X. Pan, "Biodegradable Medical Implants: Reshaping Future Medical Practice," *Advanced Science* 12, no. 35 (2025): e08014, https://doi.org/10.1002/advs.202508014.

83. B. Wan, Q. Bao, and D. Burgess, "Long-Acting PLGA Microspheres: Advances in Excipient and Product Analysis toward Improved Product Understanding," *Advanced Drug Delivery Reviews* 198 (2023): 114857, https://doi.org/10.1016/j.addr.2023.114857.

84. X. Ren, X. Gao, Y. Cheng, et al., "Maintenance of Multipotency of Bone Marrow Mesenchymal Stem Cells on Poly(epsilon-Caprolactone) Nanoneedle Arrays through the Enhancement of Cell-Cell Interaction," *Frontiers in Bioengineering and Biotechnology* 10 (2022): 1076345, https://doi.org/10.3389/fbioe.2022.1076345.

85. D. Wei, Y. Sun, H. Zhu, and Q. Fu, "Stimuli-Responsive Polymer-Based Nanosystems for Cancer Theranostics," *ACS Nano* 17, no. 23 (2023): 23223–23261, https://doi.org/10.1021/acsnano.3c06019.

86. L. Zhai, A. Narkar, and K. Ahn, "Self-Healing Polymers with Nanomaterials and Nanostructures," *Nano Today* 30 (2020): 100826, https://doi.org/10.1016/j.nantod.2019.100826.

87. J. Gan, L. Sun, W. Tang, Y. Zhao, and Y. Bi, "Separable Cryo-Microneedle Patches Delivery with Capsaicin Integrated Mesoporous Dopamine for Obesity Treatment," *Journal of Nanobiotechnology* 23, no. 1 (2025): 604, https://doi.org/10.1186/s12951-025-03645-y.

88. J. Zhang, T. Wu, Z. Wang, et al., "Plasma-Generated RONS in Liquid Transferred into Cryo-Microneedles Patch for Skin Treatment of Melanoma," *Redox Biology* 75 (2024): 103284, https://doi.org/10.1016/j.redox.2024.103284.

89. F. Milos, G. Tullii, F. Gobbo, et al., "High Aspect Ratio and Light-Sensitive Micropillars Based on a Semiconducting Polymer Optically Regulate Neuronal Growth," *ACS Applied Materials & Interfaces* 13, no. 20 (2021): 23438–23451, https://doi.org/10.1021/acsami.1c03537.

90. W. Liu, Z. Feng, W. Ou-Yang, et al., "3D Printing of Implantable Elastic PLCL Copolymer Scaffolds," *Soft Matter* 16, no. 8 (2020): 2141–2148, https://doi.org/10.1039/c9sm02396h.

91. N. Kooy, K. Mohamed, L. T. Pin, and O. S. Guan, "A Review of Roll-to-Roll Nanoimprint Lithography," *Nanoscale Research Letters* 9, no. 1 (2014): 320, https://doi.org/10.1186/1556-276X-9-320.

92. A. Dhawan, Y. Du, D. Batchelor, et al., "Hybrid Top-Down and Bottom-up Fabrication Approach for Wafer-Scale Plasmonic Nanoplatforms," *Small* 7, no. 6 (2011): 727–731, https://doi.org/10.1002/smll.201002186.

93. K. Yum, M. F. Yu, N. Wang, and Y. K. Xiang, "Biofunctionalized Nanoneedles for the Direct and Site-Selective Delivery of Probes into Living Cells," *Biochimica et Biophysica Acta (BBA) - General Subjects* 1810, no. 3 (2011): 330–338, https://doi.org/10.1016/j.bbagen.2010.05.005.

94. T. Kihara, N. Yoshida, S. Mieda, et al., "Nanoneedle Surface Modification with 2-Methacryloyloxyethyl Phosphorylcholine Polymer to Reduce Nonspecific Protein Adsorption in a Living Cell," *NanoBiotechnology* 3, no. 2 (2008): 127–134, https://doi.org/10.1007/s12030-008-9002-4.

95. C. S. Tai, K. C. Lan, E. Wang, et al., "Nanotopography as Artificial Microenvironment for Accurate Visualization of Metastasis Development via Simulation of ECM Dynamics," *Nano Letters* 21, no. 3 (2021): 1400–1411, https://doi.org/10.1021/acs.nanolett.0c04209.

96. X. Li, L. Matino, W. Zhang, et al., "A Nanostructure Platform for Live-Cell Manipulation of Membrane Curvature," *Nature Protocols* 14, no. 6 (2019): 1772–1802, https://doi.org/10.1038/s41596-019-0161-7.

97. Z. Pan, C. Yan, R. Peng, et al., "Control of Cell Nucleus Shapes via Micropillar Patterns," *Biomaterials* 33, no. 6 (2012): 1730–1735, https://doi.org/10.1016/j.biomaterials.2011.11.023.

98. L. R. Smith, S. Cho, and D. E. Discher, "Stem Cell Differentiation Is Regulated by Extracellular Matrix Mechanics," *Physiology* 33, no. 1 (2018): 16–25, https://doi.org/10.1152/physiol.00026.2017.

99. J. L. Tan, J. Tien, D. M. Pirone, et al., "Cells Lying on a Bed of Microneedles: An Approach to Isolate Mechanical Force," *Proceedings of the National Academy of Sciences of the United States of America* 100, no. 4 (2003): 1484–1489, https://doi.org/10.1073/pnas.0235407100.

100. Q. Zheng, M. Peng, Z. Liu, et al., "Dynamic Real-Time Imaging of Living Cell Traction Force by Piezo-Phototronic Light Nano-Antenna Array," *Science Advances* 7, no. 22 (2021): eabe7738, https://doi.org/10.1126/sciadv.abe7738.

101. F. Martino, A. R. Perestrelo, V. Vinarsky, S. Pagliari, and G. Forte, "Cellular Mechanotransduction: From Tension to Function," *Frontiers in Physiology* 9 (2018): 824, https://doi.org/10.3389/fphys.2018.00824.

102. K. Yang, K. Jung, E. Ko, et al., "Nanotopographical Manipulation of Focal Adhesion Formation for Enhanced Differentiation of Human Neural Stem Cells," *ACS Applied Materials & Interfaces* 5, no. 21 (2013): 10529–10540, https://doi.org/10.1021/am402156f.

103. L. U. Vinzons and S. P. Lin, "Hierarchical Micro-/Nanotopographies Patterned by Tandem Nanosphere Lens Lithography and UV-LED Photolithography for Modulating PC12 Neuronal Differentiation," *ACS Applied Nano Materials* 5, no. 5 (2022): 6935–6953, https://doi.org/10.1021/acsanm.2c00938.

104. H. K. Choi, C. H. Kim, S. N. Lee, T. H. Kim, and B. K. Oh, "Nano-Sized Graphene Oxide Coated Nanopillars on Microgroove Polymer Arrays that Enhance Skeletal Muscle Cell Differentiation," *Nano Convergence* 8, no. 1 (2021): 40, https://doi.org/10.1186/s40580-021-00291-6.

105. J. H. Lee, J. Luo, H. K. Choi, et al., "Functional Nanoarrays for Investigating Stem Cell Fate and Function," *Nanoscale* 12, no. 17 (2020): 9306–9326, https://doi.org/10.1039/c9nr10963c.

106. R. Kawamura, M. Miyazaki, K. Shimizu, et al., "A New Cell Separation Method Based on Antibody-Immobilized Nanoneedle Arrays for the Detection of Intracellular Markers," *Nano Letters* 17, no. 11 (2017): 7117–7124, https://doi.org/10.1021/acs.nanolett.7b03918.

107. Y. Wang, Y. Yang, L. Yan, et al., "Poking Cells for Efficient Vector-Free Intracellular Delivery," *Nature Communications* 5, no. 1 (2014): 4466, https://doi.org/10.1038/ncomms5466.

108. C. Xie, Z. Lin, L. Hanson, Y. Cui, and B. Cui, "Intracellular Recording of Action Potentials by Nanopillar Electroporation," *Nature Nanotechnology* 7, no. 3 (2012): 185–190, https://doi.org/10.1038/nnano.2012.8.

109. W. Zhao, L. Hanson, H. Y. Lou, et al., "Nanoscale Manipulation of Membrane Curvature for Probing Endocytosis in Live Cells," *Nature Nanotechnology* 12, no. 8 (2017): 750–756, https://doi.org/10.1038/nnano.2017.98.

110. Y. Chen, J. Wang, X. Li, et al., "Emerging Roles of 1D Vertical Nanostructures in Orchestrating Immune Cell Functions," *Advanced Materials* 32, no. 40 (2020): e2001668, https://doi.org/10.1002/adma.202001668.

111. R. Elnathan, B. Delalat, D. Brodoceanu, et al., "Maximizing Transfection Efficiency of Vertically Aligned Silicon Nanowire Arrays," *Advanced Functional Materials* 25, no. 46 (2015): 7215–7225, https://doi.org/10.1002/adfm.201503465.

112. R. Capozza, V. Caprettini, C. A. Gonano, et al., "Cell Membrane Disruption by Vertical Micro-/Nanopillars:Role of Membrane Bending and Traction Forces," *ACS Applied Materials & Interfaces* 10, no. 34 (2018): 29107–29114, https://doi.org/10.1021/acsami.8b08218.

113. S. Aslanoglou, Y. Chen, V. Oorschot, et al., "Efficient Transmission Electron Microscopy Characterization of Cell-Nanostructure Interfacial Interactions," *Journal of the American Chemical Society* 142, no. 37 (2020): 15649–15653, https://doi.org/10.1021/jacs.0c05919.

114. R. Wierzbicki, C. Kobler, M. R. Jensen, et al., "Mapping the Complex Morphology of Cell Interactions with Nanowire Substrates Using FIB-SEM," *PLoS One* 8, no. 1 (2013): e53307, https://doi.org/10.1371/journal.pone.0053307.

115. F. Santoro, W. Zhao, L. M. Joubert, et al., "Revealing the Cell-Material Interface with Nanometer Resolution by Focused Ion Beam/Scanning Electron Microscopy," *ACS Nano* 11, no. 8 (2017): 8320–8328, https://doi.org/10.1021/acsnano.7b03494.

116. C. S. Hansel, S. W. Crowder, S. Cooper, et al., "Nanoneedle-Mediated Stimulation of Cell Mechanotransduction Machinery," *ACS Nano* 13, no. 3 (2019): 2913–2926, https://doi.org/10.1021/acsnano.8b06998.

117. T. Berthing, S. Bonde, K. R. Rostgaard, et al., "Cell Membrane Conformation at Vertical Nanowire Array Interface Revealed by

Fluorescence Imaging," *Nanotechnology* 23, no. 41 (2012): 415102, https://doi.org/10.1088/0957-4484/23/41/415102.

118. J. Abbott, T. Ye, D. Ham, and H. Park, "Optimizing Nanoelectrode Arrays for Scalable Intracellular Electrophysiology," *Accounts of Chemical Research* 51, no. 3 (2018): 600–608, https://doi.org/10.1021/acs.accounts.7b00519.

119. E. Sarikhani, V. Patel, Z. Li, et al., "Engineered Nanotopographies Induce Transient Openings in the Nuclear Membrane," *Advanced Functional Materials* 35 (2024): 2410035, https://doi.org/10.1002/adfm.202410035.

120. E. A. Francis, E. Sarikhani, V. Patel, et al., "Nanoscale Curvature Regulates YAP/TAZ Nuclear Localization Through Nuclear Deformation and Rupture," *Advanced Science* 12, no. 28 (2025): e2415029, https://doi.org/10.1002/advs.202415029.

121. J. K. Kim, A. Louhghalam, G. Lee, et al., "Nuclear Lamin A/C Harnesses the Perinuclear Apical Actin Cables to Protect Nuclear Morphology," *Nature Communications* 8, no. 1 (2017): 2123, https://doi.org/10.1038/s41467-017-02217-5.

122. L. Hanson, W. Zhao, H. Y. Lou, et al., "Vertical Nanopillars for In Situ Probing of Nuclear Mechanics in Adherent Cells," *Nature Nanotechnology* 10, no. 6 (2015): 554–562, https://doi.org/10.1038/nnano.2015.88.

123. E. Sarikhani, D. P. Meganathan, K. Rahmani, et al., "*Engineering Cell and Nuclear Morphology on Nano Topography by Contact-Free Protein Micropatterning*," *preprint bioRxiv* (2023), https://doi.org/10.1101/2023.06.05.543791.

124. H. Y. Lou, W. Zhao, X. Li, et al., "Membrane Curvature Underlies Actin Reorganization in Response to Nanoscale Surface Topography," *Proceedings of the National Academy of Sciences of the United States of America* 116, no. 46 (2019): 23143–23151, https://doi.org/10.1073/pnas.1910166116.

125. X. Li, L. H. Klausen, W. Zhang, et al., "Nanoscale Surface Topography Reduces Focal Adhesions and Cell Stiffness by Enhancing Integrin Endocytosis," *Nano Letters* 21, no. 19 (2021): 8518–8526, https://doi.org/10.1021/acs.nanolett.1c01934.

126. A. J. Engler, S. Sen, H. L. Sweeney, and D. E. Discher, "Matrix Elasticity Directs Stem Cell Lineage Specification," *Cell* 126, no. 4 (2006): 677–689, https://doi.org/10.1016/j.cell.2006.06.044.

127. S. R. Caliari, S. L. Vega, M. Kwon, E. M. Soulas, and J. A. Burdick, "Dimensionality and Spreading Influence MSC YAP/TAZ Signaling in Hydrogel Environments," *Biomaterials* 103 (2016): 314–323, https://doi.org/10.1016/j.biomaterials.2016.06.061.

128. S. Dupont, L. Morsut, M. Aragona, et al., "Role of YAP/TAZ in Mechanotransduction," *Nature* 474, no. 7350 (2011): 179–183, https://doi.org/10.1038/nature10137.

129. B. C. Heng, X. Zhang, D. Aubel, et al., "Role of YAP/TAZ in Cell Lineage Fate Determination and Related Signaling Pathways," *Frontiers in Cell and Developmental Biology* 8 (2020): 735, https://doi.org/10.3389/fcell.2020.00735.

130. J. Swift, I. L. Ivanovska, A. Buxboim, et al., "Nuclear Lamin-A Scales with Tissue Stiffness and Enhances Matrix-Directed Differentiation," *Science* 341, no. 6149 (2013): 1240104, https://doi.org/10.1126/science.1240104.

131. A. Buxboim, J. Irianto, J. Swift, et al., "Coordinated Increase of Nuclear Tension and Lamin-A with Matrix Stiffness Outcompetes Lamin-B Receptor that Favors Soft Tissue Phenotypes," *Molecular Biology of the Cell* 28, no. 23 (2017): 3333–3348, https://doi.org/10.1091/mbc.E17-06-0393.

132. H. Ahn, Y. Cho, G. T. Yun, et al., "Hierarchical Topography with Tunable Micro- and Nanoarchitectonics for Highly Enhanced Cardiomyocyte Maturation via Multi-Scale Mechanotransduction," *Advanced Healthcare Materials* 12, no. 12 (2023): e2202371, https://doi.org/10.1002/adhm.202202371.

133. Z. Liu, M. Cai, X. Zhang, et al., "Cell-Traction-Triggered On-Demand Electrical Stimulation for Neuron-Like Differentiation," *Advanced Materials* 33, no. 51 (2021): e2106317, https://doi.org/10.1002/adma.202106317.

134. J. Liu, J. Jiang, M. He, et al., "Nanopore Electroporation Device for DNA Transfection into Various Spreading and Nonadherent Cell Types," *ACS Applied Materials & Interfaces* 15, no. 43 (2023): 50015–50033, https://doi.org/10.1021/acsami.3c10939.

135. Y. Liu, G. Li, T. Zhang, et al., "Driving Multifunctional Nanomedicine Design for Non-Inflammatory Tumor Therapy with Integrated Machine Learning and Density Functional Theory," *Advanced Materials* 37, no. 37 (2025): e2503576, https://doi.org/10.1002/adma.202503576.

136. D. Ren, S. Fisson, D. Dalkara, and D. Ail, "Immune Responses to Gene Editing by Viral and Non-Viral Delivery Vectors Used in Retinal Gene Therapy," *Pharmaceutics* 14, no. 9 (2022): 1973, https://doi.org/10.3390/pharmaceutics14091973.

137. K. Singh, D. Jain, P. Sethi, et al., "Advances in Viral Vector-Based Delivery Systems for Gene Therapy: A Comprehensive Review," *3 Biotech* 15, no. 7 (2025): 196, https://doi.org/10.1007/s13205-025-04366-7.

138. F. Liu, R. Su, X. Jiang, et al., "Advanced Micro/Nano-Electroporation for Gene Therapy: Recent Advances and Future Outlook," *Nanoscale* 16, no. 22 (2024): 10500–10521, https://doi.org/10.1039/d4nr01408a.

139. A. R. Shokouhi, Y. Chen, H. Z. Yoh, et al., "Electroactive Nanoinjection Platform for Intracellular Delivery and Gene Silencing," *Journal of Nanobiotechnolog* 21, no. 1 (2023): 273, https://doi.org/10.1186/s12951-023-02056-1.

140. A. R. Shokouhi, Y. Chen, H. Z. Yoh, et al., "Engineering Efficient CAR-T Cells via Electroactive Nanoinjection," *Advanced Materials* 35, no. 44 (2023): e2304122, https://doi.org/10.1002/adma.202304122.

141. V. P. Nguyen, J. Jeong, M. Zheng, et al., "Long-Term Diabetic Retinopathy Treatment Using Silicon Nanoneedles," *Small* 21, no. 9 (2025): 2410166, https://doi.org/10.1002/smll.202410166.

142. C. Samiotaki, I. Koumentakou, E. Christodoulou, et al., "Fabrication of PLA-Based Nanoneedle Patches Loaded with Transcutol-Modified Chitosan Nanoparticles for the Transdermal Delivery of Levofloxacin," *Molecules* 29, no. 18 (2024): 4289, https://doi.org/10.3390/molecules29184289.

143. Z. Wang, H. Wang, S. Lin, et al., "Efficient Delivery of Biological Cargos into Primary Cells by Electrodeposited Nanoneedles via Cell-Cycle-Dependent Endocytosis," *Nano Letters* 23, no. 13 (2023): 5877–5885, https://doi.org/10.1021/acs.nanolett.2c05083.

144. Z. B. Zhang, J. W. Zhao, Y. Q. Lei, et al., "Preparation of Intricate Nanostructures on 304 stainless Steel Surface by SiO-Assisted HF Etching for High Superhydrophobicity," *Colloids and Surfaces A: Physicochemical and Engineering Aspects* 586 (2020): 124287, https://doi.org/10.1016/j.colsurfa.2019.124287.

145. W. Zhou, Z. Zheng, C. Wang, Z. Wang, and R. An, "One-Step Fabrication of 3D Nanohierarchical Nickel Nanomace Array To Sinter with Silver NPs and the Interfacial Analysis," *ACS Applied Materials & Interfaces* 9, no. 5 (2017): 4798–4807, https://doi.org/10.1021/acsami.6b13031.

146. Y. Li, H. Zhang, R. Yang, et al., "Fabrication of Sharp Silicon Hollow Microneedles by Deep-Reactive Ion Etching towards Minimally Invasive Diagnostics," *Microsystems & Nanoengineering* 5, no. 1 (2019): 41, https://doi.org/10.1038/s41378-019-0077-y.

147. M. R. Sarabi, A. Ahmadpour, A. K. Yetisen, and S. Tasoglu, "Finger-Actuated Microneedle Array for Sampling Body Fluids," *Applied Sciences-Basel* 11, no. 12 (2021): 5329, https://doi.org/10.3390/app11125329.

148. H. Lee, C. Song, S. Baik, et al., "Device-Assisted Transdermal Drug Delivery," *Advanced Drug Delivery Reviews* 127 (2018): 35–45, https://doi.org/10.1016/j.addr.2017.08.009.

149. D. Matsumoto, R. Rao Sathuluri, Y. Kato, et al., "Oscillating High-Aspect-Ratio Monolithic Silicon Nanoneedle Array Enables Efficient Delivery of Functional Bio-Macromolecules into Living Cells," *Scientific Reports* 5, no. 1 (2015): 15325, https://doi.org/10.1038/srep15325.

150. J. Casper, S. H. Schenk, E. Parhizkar, et al., "Polyethylenimine (PEI) in Gene Therapy: Current Status and Clinical Applications," *Journal of Controlled Release* 362 (2023): 667–691, https://doi.org/10.1016/j.jconrel.2023.09.001.

151. K. Wong, G. Sun, X. Zhang, et al., "PEI-g-Chitosan, a Novel Gene Delivery System with Transfection Efficiency Comparable to Polyethylenimine In Vitro and after Liver Administration In Vivo," *Bioconjugate Chemistry* 17, no. 1 (2006): 152–158, https://doi.org/10.1021/bc0501597.

152. M. Kanamala, W. R. Wilson, M. Yang, B. D. Palmer, and Z. Wu, "Mechanisms and Biomaterials in pH-Responsive Tumour Targeted Drug Delivery: A Review," *Biomaterials* 85 (2016): 152–167, https://doi.org/10.1016/j.biomaterials.2016.01.061.

153. A. Ullah, H. Khan, H. J. Choi, and G. M. Kim, "Smart Microneedles with Porous Polymer Coatings for pH-Responsive Drug Delivery," *Polymers* 11, no. 11 (2019): 1834, https://doi.org/10.3390/polym11111834.

154. S. Zhang, B. Dong, Y. Shuai, et al., "Enzyme-Responsive Peptide-Prodrug Integrated Biphasic Microneedle Patch for Enhanced Transdermal Delivery and Hypertension Therapy," *ACS Applied Materials & Interfaces* 17, no. 34 (2025): 47857–47868, https://doi.org/10.1021/acsami.5c06128.

155. H. Kim, H. Lee, K. Y. Seong, et al., "Visible Light-Triggered On-Demand Drug Release From Hybrid Hydrogels and Its Application in Transdermal Patches," *Advanced Healthcare Materials* 4, no. 14 (2015): 2071–2077, https://doi.org/10.1002/adhm.201500323.

156. W. Y. Jeong, M. Kwon, H. E. Choi, and K. S. Kim, "Recent Advances in Transdermal Drug Delivery Systems: A Review," *Biomaterials Research* 25, no. 1 (2021): 24, https://doi.org/10.1186/s40824-021-00226-6.

157. Y. Zhang, Y. Xu, H. Kong, et al., "Microneedle System for Tissue Engineering and Regenerative Medicine," *Exploration* 3, no. 1 (2023): 20210170, https://doi.org/10.1002/EXP.20210170.

158. S. Hu, M. Zhu, H. Xing, et al., "Thread-Structural Microneedles Loaded with Engineered Exosomes for Annulus Fibrosus Repair by Regulating Mitophagy Recovery and Extracellular Matrix Homeostasis," *Bioactive Materials* 37 (2024): 1–13, https://doi.org/10.1016/j.bioactmat.2024.03.006.

159. C. Chiappini, "Nanoneedle-Based Sensing in Biological Systems," *ACS Sensors* 2, no. 8 (2017): 1086–1102, https://doi.org/10.1021/acssensors.7b00350.

160. Y. Cho, Y. Choi, Y. Jang, and H. Seong, "Nanomaterial-Enhanced Biosensing: Mechanisms and Emerging Applications," *Advanced Healthcare Materials* 14, no. 31 (2025): e2500189, https://doi.org/10.1002/adhm.202500189.

161. R. Kawamura, K. Shimizu, Y. Matsumoto, et al., "High Efficiency Penetration of Antibody-Immobilized Nanoneedle Thorough Plasma Membrane for In Situ Detection of Cytoskeletal Proteins in Living Cells," *Journal of Nanobiotechnology* 14, no. 1 (2016): 74, https://doi.org/10.1186/s12951-016-0226-5.

162. C. Chiappini, P. Campagnolo, C. S. Almeida, et al., "Mapping Local Cytosolic Enzymatic Activity in Human Esophageal Mucosa with Porous Silicon Nanoneedles," *Advanced Materials* 27, no. 35 (2015): 5147–5152, https://doi.org/10.1002/adma.201501304.

163. W. Park, E. M. Kim, Y. Jeon, et al., "Transparent Intracellular Sensing Platform with Si Needles for Simultaneous Live Imaging," *ACS Nano* 17, no. 24 (2023): 25014–25026, https://doi.org/10.1021/acsnano.3c07527.

164. J. Abbott, T. Ye, L. Qin, et al., "CMOS Nanoelectrode Array for All-Electrical Intracellular Electrophysiological Imaging," *Nature Nanotechnology* 12, no. 5 (2017): 460–466, https://doi.org/10.1038/nnano.2017.3.

165. M. Sang, M. Cho, S. Lim, et al., "Fluorescent-Based Biodegradable Microneedle Sensor Array for Tether-Free Continuous Glucose Monitoring with Smartphone Application," *Science Advances* 9, no. 22 (2023): eadh1765, https://doi.org/10.1126/sciadv.adh1765.

166. Y. Hu, E. Chatzilakou, Z. Pan, G. Traverso, and A. K. Yetisen, "Microneedle Sensors for Point-of-Care Diagnostics," *Advanced Science* 11, no. 12 (2024): e2306560, https://doi.org/10.1002/advs.202306560.

167. W. Lee, S. H. Jeong, Y. W. Lim, et al., "Conformable Microneedle pH Sensors via the Integration of Two Different Siloxane Polymers for Mapping Peripheral Artery Disease," *Science Advances* 7, no. 48 (2021): eabi6290, https://doi.org/10.1126/sciadv.abi6290.

168. K. Y. Goud, C. Moonla, R. K. Mishra, et al., "Wearable Electrochemical Microneedle Sensor for Continuous Monitoring of Levodopa: Toward Parkinson Management," *ACS Sensors* 4, no. 8 (2019): 2196–2204, https://doi.org/10.1021/acssensors.9b01127.

169. J. Xiao, S. Zhang, Q. Liu, T. Xu, and X. Zhang, "Microfluidic-Based Plasmonic Microneedle Biosensor for Uric Acid Ultrasensitive Monitoring," *Sensors and Actuators B: Chemical* 398 (2024): 134685, https://doi.org/10.1016/j.snb.2023.134685.

170. X. Yu, H. Wang, X. Ning, et al., "Needle-Shaped Ultrathin Piezoelectric Microsystem for Guided Tissue Targeting via Mechanical Sensing," *Nature Biomedical Engineering* 2, no. 3 (2018): 165–172, https://doi.org/10.1038/s41551-018-0201-6.

171. R. Ghosh, M. S. Song, J. Park, et al., "Fabrication of Piezoresistive Si Nanorod-Based Pressure Sensor Arrays: A Promising Candidate for Portable Breath Monitoring Devices," *Nano Energy* 80 (2021): 105537, https://doi.org/10.1016/j.nanoen.2020.105537.

172. Y. Li, C. Lin, Y. Peng, J. He, and Y. Yang, "High-Sensitivity and Point-of-Care Detection of SARS-CoV-2 From Nasal and Throat Swabs by Magnetic SERS Biosensor," *Sensors and Actuators B: Chemical* 365 (2022): 131974, https://doi.org/10.1016/j.snb.2022.131974.

173. M. Guo, Y. Wang, B. Gao, and B. He, "Shark Tooth-Inspired Microneedle Dressing for Intelligent Wound Management," *ACS Nano* 15, no. 9 (2021): 15316–15327, https://doi.org/10.1021/acsnano.1c06279.

174. J. Kang, K. Y. Kim, S. Kim, et al., "A Conformable Microneedle Sensor with Photopatternable Skin Adhesive and Gel Electrolyte for Continuous Glucose Monitoring," *Device* 1, no. 4 (2023): 100112, https://doi.org/10.1016/j.device.2023.100112.

175. K. Stokes, K. Clark, D. Odetade, M. Hardy, and P. Goldberg Oppenheimer, "Advances in Lithographic Techniques for Precision Nanostructure Fabrication in Biomedical Applications," *Discover Nano* 18, no. 1 (2023): 153, https://doi.org/10.1186/s11671-023-03938-x.

176. C. F. Rodriguez, V. Andrade-Perez, M. C. Vargas, et al., "Breaking the Clean Room Barrier: Exploring Low-Cost Alternatives for Microfluidic Devices," *Frontiers in Bioengineering and Biotechnology* 11 (2023): 1176557, https://doi.org/10.3389/fbioe.2023.1176557.

177. T. Liu, Y. Sun, W. Zhang, et al., "Mechanical Investigation of Solid MNs Penetration into Skin Using Finite Element Analysis," *Advanced Engineering Materials* 26, no. 5 (2023): 2301532, https://doi.org/10.1002/adem.202301532.

178. C. Song, Z. Zhao, Y. Lin, et al., "A Nanoneedle-Based Reactional Wettability Variation Sensor Array for on-Site Detection of Metal Ions with a Smartphone," *Journal of Colloid and Interface Science* 547 (2019): 330–338, https://doi.org/10.1016/j.jcis.2019.04.015.

179. M. V. Singh, P. Apshingekar, S. Gandhi, and O. V. Singh, "US Regulatory Compliance for Medical Combination Products: An Overview," *Frontiers in Medical Technology* 6 (2024): 1486318, https://doi.org/10.3389/fmedt.2024.1486318.

180. D. K. Gupta, A. Tiwari, Y. Yadav, P. Soni, and M. Joshi, "Ensuring Safety and Efficacy in Combination Products: Regulatory Challenges and Best Practices," *Frontiers in Medical Technology* 6 (2024): 1377443, https://doi.org/10.3389/fmedt.2024.1377443.

181. G. D'Avenio, C. Daniele, and M. Grigioni, "Nanostructured Medical Devices: Regulatory Perspective and Current Applications," *Materials* 17, no. 8 (2024): 1787, https://doi.org/10.3390/ma17081787.

182. Z. Jiang, W. Wu, T. Chen, et al., "Barrier-Disrupting Microneedle Technology: Overcoming Physical, Physiological, and Pathological Skin Defenses to Enhance Therapeutic Efficacy," *Bioactive Materials* 57 (2026): 400–429, https://doi.org/10.1016/j.bioactmat.2025.11.005.

183. J. C. J. Wei, G. A. Edwards, D. J. Martin, et al., "Allometric Scaling of Skin Thickness, Elasticity, Viscoelasticity to Mass for Micro-Medical Device Translation: From Mice, Rats, Rabbits, Pigs to Humans," *Scientific Reports* 7, no. 1 (2017): 15885, https://doi.org/10.1038/s41598-017-15830-7.

184. R. Bosetti and S. L. Jones, "Cost-Effectiveness of Nanomedicine: Estimating the Real Size of Nano-Costs," *Nanomedicine* 14, no. 11 (2019): 1367–1370, https://doi.org/10.2217/nnm-2019-0130.

Biographies

Yerim Jang is a doctoral student in the Department of Chemical and Biomolecular Engineering at the Korea Advanced Institute of Science and Technology. She received her M.S. degree in Nano-Bio-Information Technology from the KU-KIST Graduate School of Converging Science and Technology in 2024. Her research interests include cell–material interfaces and nanomaterial-based bioengineering.

Sowon Lee is a master's student in the School of Biomedical Engineering at Korea University. Her research interests include nanoneedle-based intracellular delivery and surface characterization for bioengineering applications.

Younghak Cho received his B.S. (2015) and Ph.D. (2022) degrees in Chemical and Biomolecular Engineering from Korea Advanced Institute of Science and Technology. He currently works as a research scientist at the Stem Cell Convergence Research Center, Division of Research on National Challenges, Korea Research Institute of Bioscience and Biotechnology (KRIBB). His research interests center on organoid engineering and 3D tissue systems.

Hyejeong Seong received her B.S. (2007) and Ph.D. (2016) degrees in Chemical and Biomolecular Engineering from Korea Advanced Institute of Science and Technology. She worked as a Research Associate in the Stevens Group at Imperial College London from 2017 to 2020. Currently, she is a Senior Researcher in the Brain Science Institute at Korea Institute of Science and Technology. Her accolades include a Marie Skłodowska-Curie Fellowship from the European Union, and an NRF-Fellowship from Republic of Korea. Her research interests focus on microfabrication of biomaterials for cell-interfacing applications and biosensors.